WATER RESOURCES RESEARCH, VOL. 36, NO. 7, PAGES 1845–1863, JULY 2000

Conservation equations governing hillslope responses: Exploring the physical basis of water balance

Paolo Reggiani and Murugesu Sivapalan

Centre for Water Research, Department of Environmental Engineering, University of Western Australia, Nedlands, Australia

S. Majid Hassanizadeh

Section for Hydrology and Ecology, Faculty of Civil Engineering and Geosciences, Delft University of Technology, Delft, Netherlands

Abstract. A unifying approach for the derivation of watershed-scale conservation equations governing hydrologic responses has recently been introduced. The approach is based on space-time averaging of the corresponding point-scale conservation equations over an averaging region called the representative elementary watershed (REW). The conservation equations are supplemented by constitutive relationships needed for the closure of various mass and momentum exchange terms. In this paper, we present a summary of the resulting equations for a somewhat simpler problem and show how these equations can be employed to model the long-term water balance of a single, hypothetical REW. The governing equations are formulated in terms of an average saturation and a flow velocity of the unsaturated zone soils and the average thickness of the saturated zone soils. The equations are coupled ordinary differential equations and are nonlinear. Their solution is carried out simultaneously for a variety of combinations of watershed geometry, soil type, and atmospheric forcing. We show how a similarity analysis of the governing equations can lead to a general classification of REWs in terms of meaningful dimensionless similarity variables. In addition, we investigate the long-term water balance and show that the governing equations are able to provide a realistic picture of the impact of changing climate, soil, and topographic controls on long-term water balance.

1. Introduction

Previously, *Reggiani et al*. [1998, 1999a] developed a mathematical framework for watershed thermodynamics with the idea that it could henceforth form the theoretical basis for watershed modeling and measurement. The goal of this paper is to demonstrate, through a simple theoretical exercise, how the above mentioned thermodynamic framework can be employed to model fundamental characteristics of catchment water balance. In this context, we make a series of assumptions with respect to soil properties, system geometry, and atmospheric forcing, which are stated clearly at the outset. For example, spatial variability of soils and climate are ignored, as a first step. Then, through the use of a simple numerical model based on the above theory, the climate, soil, and topographic controls on the annual water budget of a hypothetical watershed entity are explored. We must emphasize that the results thus obtained depend critically on the assumed forms for a number of constitutive relationships that appear in the balance equations and on their assumed parameterizations. These assumed relationships represent preliminary approximations, which require further extension and validation through carefully planned field experiments and fine-scale numerical modeling. The strength of our approach is that it is possible to go back and relax any of these assumptions if deemed necessary for a particular situation.

Paper number 2000WR900066.
0043-1397/00/2000WR900066$09.00

The crucial factors determining the long-term water balance of an unvegetated hillslope or watershed entity can be summarized as topography, soils, and atmospheric forcing. Much of our current understanding of the dynamics of water balance derives from the pioneering work of *Eagleson* [1978a, b, c, d], who investigated climate-soil-vegetation controls on water balance using one-dimensional (vertical) models of infiltration and evapotranspiration. However, Eagleson's work ignored topographic effects controlling both surface runoff by saturation excess and subsurface runoff (drainage). In contrast to Eagleson, *Milly* [1994] investigated process controls on observed spatial patterns of annual water balance but hypothesized that finite storage capacity of soils (not permeability) had the biggest control on water balance. Milly also investigated the effects of seasonality and storminess but did not include the effects of vegetation or its spatial variability. More recently, *Salvucci and Entekhabi* [1995] extended the work of Eagleson by simulating the hydrologic fluxes on idealized hillslopes, by focusing especially on topographic controls. In this case, they used a spatially distributed model of hillslope hydrology, as an extension to Eagleson's work. They worked with a range of soil thicknesses, slope angles, convergence or divergence features, climatic forcing patterns, and soil characteristics. They were able to predict long-term mean or equilibrium water table profiles below the soil surface and net recharge and discharge areas for given topographic, climatic, and pedologic circumstances. However, they too, did not include vegetation effects.

The mathematical framework derived by *Reggiani et al*. [1998, 1999a] comprises the derivation of watershed-scale bal-

ance equations for mass, momentum, energy, and entropy for fundamental watershed entities, called representative elementary watersheds (REWs), by means of averaging of the corresponding point-scale conservation laws in space and time. The REWs constitute "cells," forming basic discretization units for a complete watershed. Each REW includes an ensemble of five zero-dimensional subregions: unsaturated zone, saturated zone, channel, saturated overland flow, and concentrated overland flow. For each of these subregions all associated variables and properties are spatially lumped quantities and can vary only in time. The governing equations form a set of coupled ordinary differential equations (ODEs), which simplify the description of the system significantly, while incorporating the physics which govern the flow. The averaging procedure also generates watershed-scale exchange terms for mass and forces among the REWs and between the subregions within each REW. These exchange terms constitute unknowns of the problem. Constitutive relationships, which relate mass fluxes and exchanges of pressure forces to average quantities of the system (saturation, water table depth, velocity, topography, soil properties, etc.), need to be developed to complement the balance equations. This task, commonly known as closure, has been carried out by *Reggiani et al*. [1999a] in a systematic manner with the aid of the *Coleman and Noll* [1963] procedure, which makes use of the second law of thermodynamics as a constraint. Recently, a numerical exercise involving the solution of the watershed-scale balance equations for the channel network of a natural watershed has been pursued by *Reggiani et al*. [1999b].

We emphasize that the use of the second law of thermodynamics for the derivation of constitutive relationships could have been circumvented by postulating expressions for the closure schemes directly in an ad hoc manner based purely on physical intuition. However, the exploitation of a classical physical principle such as the second law provides a consistent qualitative tool, which has been shown to lead to well-known results, even in situations where physical intuition does not exist or is suspect. This is the case in watershed hydrology. As such, it provides a systematic and consistent procedure for the derivation of various constitutive parameterizations for the various components of an entire watershed hydrological system. In the process of developing the theory for practical applications, we will, of course, make a number of simplifying assumptions. Nevertheless, the physical basis of the theory will always be preserved.

The work of *Duffy* [1996] is similar in some respects to the work presented in this paper. Duffy introduced a hillslope model, separating the subsurface zone into saturated and unsaturated stores, which interact through mass fluxes across the water table. Constitutive relationships for the mass exchange terms were, however, postulated without recourse to the momentum and energy balances. The parameter values in these constitutive relations were obtained by matching them with the results obtained from a finite element Richards equation solver. Duffy looked at long-term water balance equilibria as well as at individual storm responses.

In this paper, we consider a numerical application for a hypothetical system consisting of a single, isolated REW. However, to keep the problem simple and to avoid processes covering a diverse range of timescales, we concentrate our attention on only two subregions of the REW (the unsaturated and saturated zones) and ignore overland flow and channel flow processes. The numerical exercise thus consists of the simultaneous solution of the conservation equations for mass within the unsaturated and saturated zones, with a watershed-scale Darcy's law (representing momentum balance), which is derived as part of the theory, governing the vertical flow velocity across the unsaturated zone. We use the numerical model developed as part of this application to investigate the theoretical basis of water balance, especially the climatic, soil, and topographic controls on annual water budgets.

We begin with a definition of the problem being studied, including the problem geometry (the features of the REW being considered), the assumed soil properties, and the atmospheric forcing. The averaged balance laws are presented next and are taken from the more comprehensive derivations of *Reggiani et al*. [1998]. The closure schemes used for the various mass and force exchange terms are presented in section 4. These are taken from *Reggiani et al*. [1999a], along with particular forms chosen to reflect the specific problem considered here. To aid us in this investigation, the derived governing equations are recast into dimensionless forms, yielding a set of dimensionless "similarity" parameters, which capture the interactions among climate, soil properties, and topography (flatness or steepness). The nondimensional form of the resulting set of balance equations and the numerical algorithms adopted to solve them are presented in sections 5 and 6. Finally, the resulting numerical model is used to investigate the climatic, soil, and topographic controls on annual water balance by carrying out sensitivity analyses with respect to the key dimensionless similarity variables mentioned above. The results and their interpretation are discussed in section 4. The paper concludes with a discussion of the limitations of the outlined approach and the results obtained. It also proposes topics of further research required for a comprehensive investigation of long-term water balance, in particular, and the physically based modeling of watershed responses, in general, especially over a variety of timescales.

2. Definition of the Problem

In this section we introduce the three fundamental components controlling the long-term water balance within an REW in the absence of vegetation. These are geometry (or topography), soil type, and atmospheric forcing. We address each single factor separately. First, we point out the main geometric quantities deemed necessary for the description of the REW. These have already been defined during the averaging procedure (for reference, see *Reggiani et al*. [1998, 1999a]) and are only briefly revisited here. Next, we point out how we incorporate soil properties into the balance equations and present the assumptions underlying their application. In this context we again emphasize that nothing prevents us from relaxing these assumptions in future applications. Finally, we explain how we drive the system through atmospheric forcing and the way in which we capture the long-term averages of the typical meteorological inputs (rainfall and potential evapotranspiration) and their representative timescales.

2.1. Geometry

The balance equations for mass and momentum will be solved for a watershed entity comprising the saturated and the unsaturated zones. According to the definitions given by *Reggiani et al*. [1998] a REW constitutes a complete subwatershed, as shown in Figure 1, including the subsurface (unsaturated and saturated zones), saturated and concentrated overland

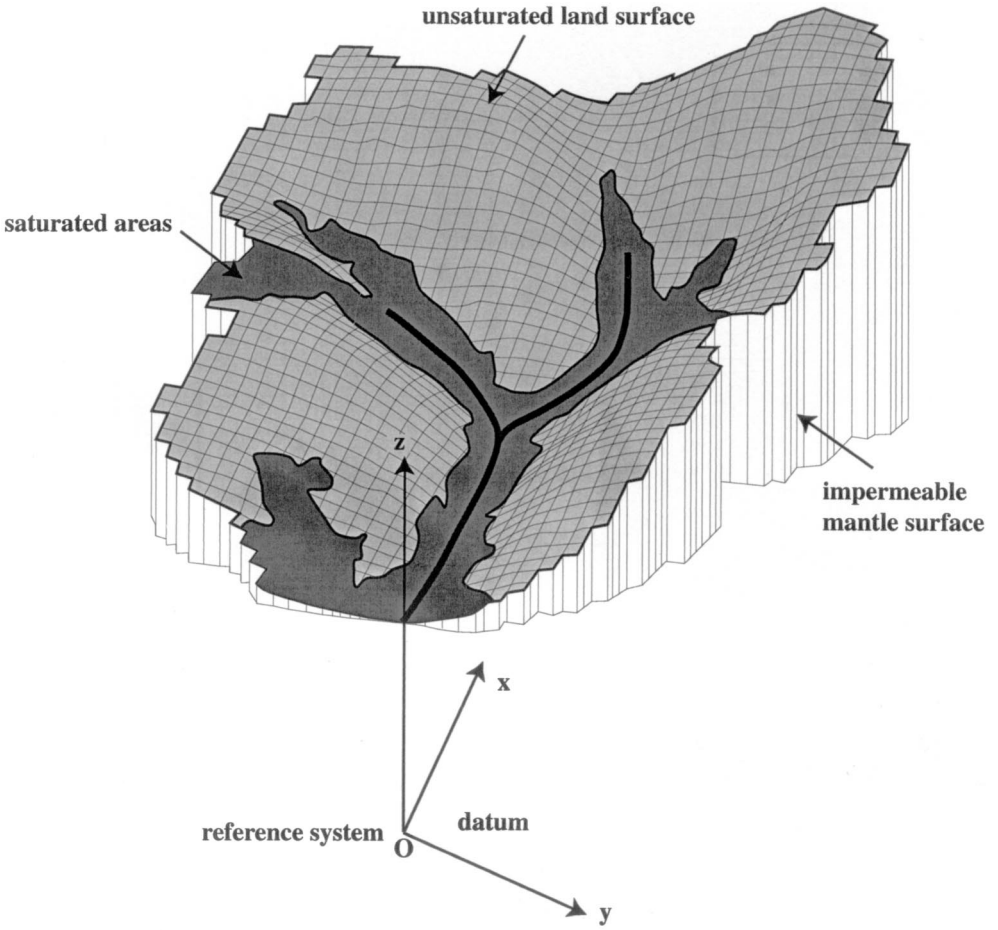

Figure 1. Three-dimensional view of watershed and the global reference system.

flow zones, and a river channel. For the purposes of water balance analysis pursued here, we consider the REW as isolated from neighboring REWs and ignore the dynamics of both overland flow zones and the channel flow. This is equivalent to stating that no mass is transferred across the prismatic mantle surface delimiting the REW laterally.

A Cartesian reference system is positioned at the outlet of the REW, as depicted in Figure 1. The x and y axes form a horizontal plane parallel to the boundary delimiting the REW at the bottom. The zero elevation mark is assumed to coincide with an arbitrary reference datum. Owing to the fact that the REW is considered here in isolation, not in relation to surrounding REWs, the x and the y axes can have an arbitrary orientation around the z axis. Furthermore, we introduce three unit vectors, pointing along the axes of the reference system, $\mathbf{e}_x$, $\mathbf{e}_y$, and $\mathbf{e}_z$, respectively.

The actual system shown in Figure 1 is replaced, through the averaging process, by a single lumped cell, as shown in Figure 2. The REW is confined at the bottom by an impermeable boundary, with an average elevation z^s above the datum, and covers a land surface area S whose projection onto the horizontal plane is denoted with Σ, as shown in Figure 2. A single average depth y^s is associated with the aquifer, while the unsaturated zone measures an average thickness y^u. Both quantities y^u and y^s are related to each other through the relationship (B1) in Appendix B.

The water table intersects the land surface in the lowest parts of the REW, forming saturated areas or seepage faces covering a surface area S^o. The projection of S^o onto the horizontal plane is denoted with Σ^o, while the projection of the unsaturated and saturated zones onto the horizontal are labelled with Σ^u and Σ^s (see Figure 2). Area fractions ω^o, ω^u, and ω^s are associated with the seepage faces, the unsaturated and the saturated zones:

$$\omega^j = \Sigma^j/\Sigma; \qquad j = o, u, s. \tag{1}$$

The area fractions are measurable watershed-scale quantities. The seepage faces are wrapped around a channel which drains the REW toward the outlet at the lowest point of the REW boundary and act, in the lumped system of Figure 2, as a point sink for the saturated zone.

We assume that the closed shape of the mantle, delimiting the system laterally, causes all pressure forces acting on the mantle to cancel each other, yielding a zero average horizontal flow within the REW. This consideration will render the use of the conservation equations for horizontal momentum within the REW redundant and only the momentum equations along the vertical will be considered. This aspect will be explained in terms of the governing equations in section 3. For the proposed application we consider the overland flow areas and the channel to be hydrologically inactive. This is equivalent to the assumption that the channel and overland flow subregions have negligible storage capacities. This is a reasonable assumption for long-term water balance investigations in view of the short timescales of the overland and channel flow subregions, relative to the subsurface soil zones. It also serves to simplify

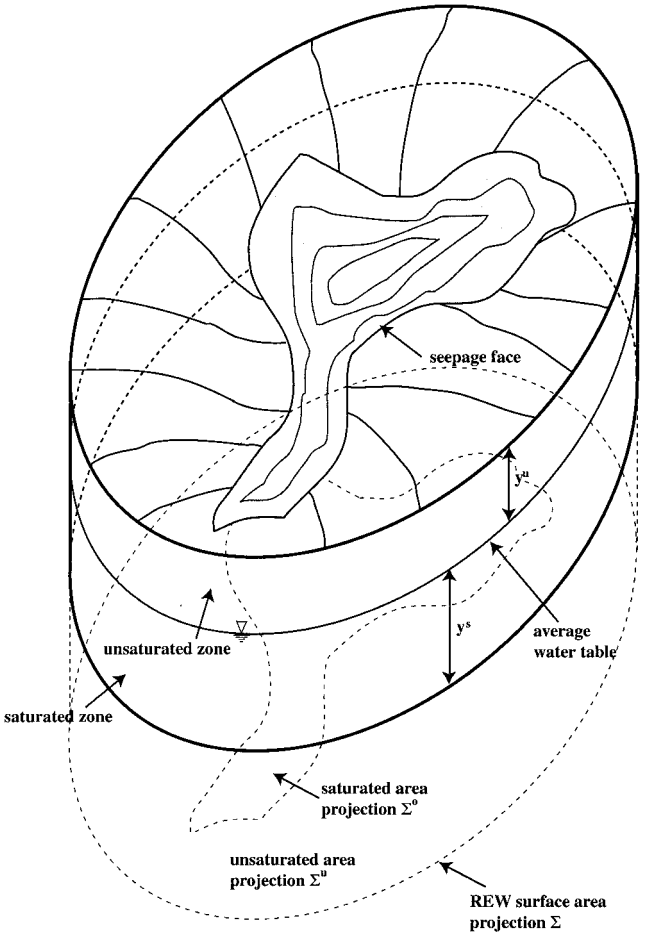

Figure 2. Lumped system representation and definition of variables.

the problem considerably. Nevertheless, it is necessary to assign an average elevation z^r to the channel bed with respect to the common datum. We also need to associate average center of mass elevations with the unsaturated and saturated zones, the seepage faces, and the unsaturated land surface. With reference to Figure 3 the center of mass elevation of the saturated zone is defined as

$$\zeta^s = \tfrac{1}{2}y^s + z^s, \tag{2}$$

while the center of mass elevation for the unsaturated zone is given by the sum of the absolute elevation of the average water table ($y^s + z^s$) plus half of the unsaturated zone thickness:

$$\zeta^u = \tfrac{1}{2}y^u + y^s + z^s. \tag{3}$$

The center of mass elevation of the saturated overland flow is derived by considering that the average vertical thickness of the flow sheet is negligible with respect to all other quantities ($y^o \approx 0$):

$$\zeta^o = \tfrac{1}{2}y^o + \tfrac{1}{2}(y^s + z^s - z^r) + z^r \approx \tfrac{1}{2}(y^s + z^s + z^r). \tag{4}$$

The average center of mass elevation for the unsaturated portion of the land surface, under the assumption of no or negligible ponded water on the surface ($y^c \approx 0$), can be given as

$$\zeta^c = y^u + y^s + z^s. \tag{5}$$

The average center of mass elevation of the channel is assumed to coincide with its average bed elevation:

$$\zeta^r = z^r. \tag{6}$$

The outlined quantities are all shown on Figure 3, depicting a typical cross section of the REW. Figure 3 also illustrates the relevant mass fluxes and pressure forces acting within the components of the system.

2.2. Soil Type

For the characterization of the soil types we refer to common approaches adopted in soil physics. Generally, soil types are characterized by a pore-disconnectedness index λ and a pore-size distribution index μ. In addition, the porosity ε is necessary for complete characterization of the soil types. *Brooks and Corey* [1966] proposed empirical expressions relating the capillary pressure in the unsaturated soils to the saturation s defined as the ratio of the volume of pore water over volume of voids:

$$p_{\text{cap}}(s) = \rho g \psi_b s^{-1/\mu}, \tag{7}$$

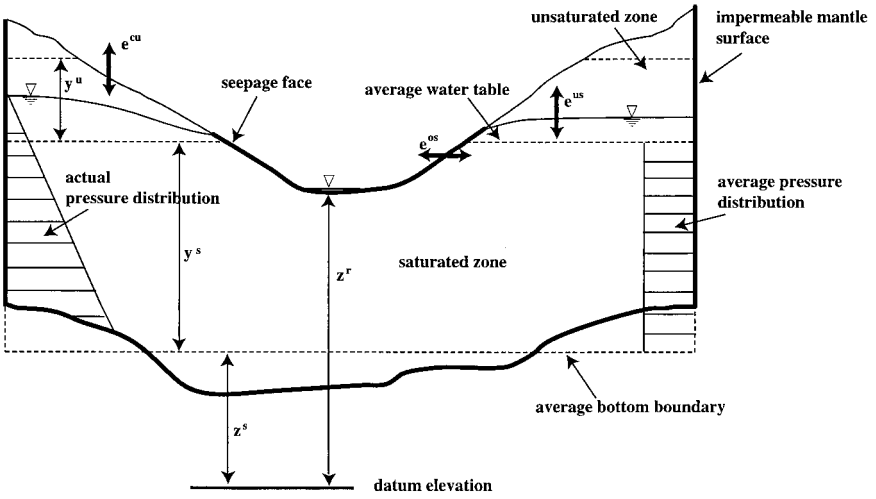

Figure 3. Vertical transect across the REW and definition of variables.

where p_{cap} is the capillary pressure and ψ_b $[L]$ is the air entry (or bubbling) capillary pressure head. The effective hydraulic conductivity $K(s)$ in the unsaturated zone under unsaturated conditions ($s < 1$) can be related to the saturated hydraulic conductivity K_{sat} via the relationship

$$K(s) = K_{sat} s^{\lambda}. \tag{8}$$

The two indices λ and μ can be reconciled by integrating the simplified *Burdine* [1958] equation governing the relationship between permeability and capillary pressure:

$$\lambda = 3 + 2/\mu. \tag{9}$$

However, (7) and (8) are point-scale equations and will apply to our situation only if the soils in the subsurface zone can be assumed to be uniform. For heterogeneous soils the above relationships will change from point to point within the REW. In our approach the details of such heterogeneity within the unsaturated and saturated subsurface zones of a REW cannot be explicitly modeled, and their effects must therefore be parameterized. In other words, all variables and parameters used must be REW-scale quantities, which then cannot vary within the REW or the soil profile. As we will show in section 3, the saturation value in the unsaturated zone is represented in the lumped system of Figure 2 by a spatial average value s^u to be evaluated from the mass balance equation (11). Similarly average values for water pressure and capillary pressure are defined and used. Thus, in principle, even if equations (7) and (8) hold in smaller, uniform regions within the unsaturated zone, they may not hold at the REW scale. Nevertheless, a dependence of the REW-scale capillary pressure on the mean saturation s^u is to be expected. In order to account for the lumped effect of other small-scale heterogeneities a dependence on other mean properties may also be required. One plausible relationship, for example, is

$$p_{cap} = p_{cap}(s^u, y^u). \tag{10}$$

At this stage, however, we do not have any concrete field information to independently parameterize such a relationship for use in modeling. In the absence of such information, for the purposes of the numerical study reported in sections 6 and 7 we assume that (7) and (8) continue to hold at the REW scale. Some typical soil parameter values are given in Table 1.

Further investigations through detailed field experiments and/or flow simulations using physically based numerical models on a fine grid need to be carried out in order to determine a more realistic REW-scale relationship between capillary pressure and saturation (and any other state variable), incorporating the effects of sub-REW-scale variability. This is left for further study.

2.3. Atmospheric Forcing

In previous studies of a similar nature [e.g., *Eagleson*, 1978a] it has been customary to consider the rainfall inputs as a Poisson arrival process of independent rainfall events whose durations are exponentially distributed, with constant intensities (i.e., rectangular pulses) drawn from either an exponential or a gamma distribution. For simplicity, in this paper, we ignore the stochastic nature of atmospheric forcing in favor of a deterministic approach and consider the rainfall inputs as a series of identical storms, with duration τ_r $[T]$, average intensity ι $[L/T]$, and an interstorm period τ_b $[T]$, characterized by a constant rate of potential evaporation e_p $[L/T]$, all set to their long-term average values. This is similar to the approach employed by *Robinson and Sivapalan* [1997]. For such an application the mean storm intensity $i = E[\iota]$, mean storm duration $t_r = E[\tau_r]$, and mean interstorm period $t_b = E[\tau_b]$ can be estimated from rainfall data taken from representative or actual locations and taken over appropriately long observation periods. The potential evaporation e_p is, in practice, dictated by factors such as air temperature, wind speed, humidity, solar radiation, cloud cover, and albedo of the soil surface. In this paper, e_p is assumed to be a known quantity to be prescribed externally, a common assumption throughout the hydrological literature [e.g., *Eagleson*, 1978a, b; *Salvucci and Entekhabi*, 1995].

Representative values of the mean climatic quantities, along with the total mean annual evapotranspiration E_{P_A} and the total mean annual precipitation P_A, are reported in Table 2 for three different climate regimes. As mentioned before, we assume that the system is forced periodically by identical rectangular pulses of rainfall of constant duration t_r and constant intensity i followed by interstorm periods of constant duration t_b characterized by a constant potential evaporation rate e_p, as shown in Figure 4. This permits us to capture the long-term water balance by studying the response of the watershed over a single forcing cycle (i.e., consisting of a single storm period and the consecutive single, interstorm period) since under steady state conditions the response of each such cycle is identical. This simple representation of atmospheric forcing is subject to obvious limitations based on the fact that seasonal variations and forms of random rainfall variability (for refer-

Table 1. Soil Parameters

Soil Type	ψ_b, m	K_{sat}, m s^{-1}	ε	λ	μ
Silty loam	0.45	3.4×10^{-6}	0.35	4.7	1.2
Sandy loam	0.25	3.4×10^{-5}	0.25	3.6	3.3
Sand	0.15	3.4×10^{-3}	0.20	3.4	5.4

From *Bras* [1990].

Table 2. Climate Parameters

Climate	t_b, days	t_r, days	i, cm d^{-1}	e_p, cm d^{-1}	P_A, cm yr^{-1}	E_{P_A}, cm yr^{-1}
Humid	3.77	0.72	1.61	0.19	94.2	58.2
Semihumid	3.44	0.25	5.07	0.33	125.4	112.3
Arid	2.99	0.48	6.46	0.41	75.5	139.3

After *Hawk and Eagleson* [1992] and *Salvucci and Entekhadi* [1994].

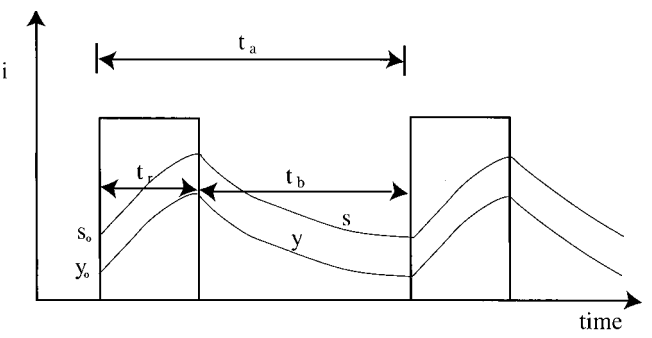

Figure 4. Climatic forcing cycle used in the simulations.

ence, see, e.g., *Eagleson* [1978a] and *Milly* [1994]) have been ignored. Nevertheless, we submit that for testing the applicability of our theory the simple representation of climate forcing described above is adequate. Future work can investigate the effects of seasonality of climatic inputs and the randomness of storm and interstorm climatic forcing. Similarly, the spatial variability of rainfall within the watershed will be resolved at the REW scale. Any smaller-scale variability will have to be parameterized and not explicitly included.

3. Governing Equations

REW-scale conservation laws for mass, momentum, energy, and entropy for the five subregions occupying the REW have been derived rigorously by *Reggiani et al*. [1999a]. In this paper, we are interested in the investigation of annual water balance. As shown by *Dunne* [1978], the characteristic timescales associated with the flows in the subsurface zones exceed those associated with the surface flows (overland flow and channel flow) by some orders of magnitude. Therefore their dynamics do not need to be explicitly modeled for water balance investigations. Thus only the equations governing flow in the two subsurface zones will be presented in this paper, namely, the unsaturated and saturated soil zones. Those exchange terms for mass and forces, which are not relevant in this paper, have been omitted. Thermal balances associated with the description of evapotranspiration of soil water are also neglected at this stage. Consequently, we ignore balance equations of energy and only report the conservation laws for mass and momentum. Once again, we point out that these assumptions can be relaxed any time in future applications. We note also that the equations are expressed on a per-unit-area basis and are therefore normalized with respect to Σ.

3.1. Unsaturated Zone Mass Conservation

The conservation of mass for the water phase in the unsaturated zone, as derived by *Reggiani et al*. [1998] is given next. With reference to Figures 2 and 3 we state that

$$\frac{d}{dt}(\rho\varepsilon s^u y^u \omega^u) = e^{us} + e^{uc} + e^u_{wg}, \tag{11}$$

where ρ is the water density, y^u is the average vertical thickness of the unsaturated zone, ε is the average porosity of the soil matrix, s^u is the average water phase saturation, and ω^u is the fraction of horizontal watershed area covered by the unsaturated zone. The mass exchange terms represent the recharge to or the capillary rise from the saturated zone, e^{us} $[M/TL]$, the infiltration from the land surface, e^{uc}, and the water phase evaporation within the soil pores, e^u_{wg}.

3.2. Saturated Zone Mass Conservation

In analogy to (11) the water mass balance for the saturated zone of the REW is

$$\frac{d}{dt}(\rho\varepsilon y^s \omega^s) = e^{su} + e^{so}, \tag{12}$$

where y^s is the average vertical thickness of the saturated zone. The right-hand side terms are the mass flux across the water table (recharge and capillary rise), e^{su}, and the flux across the seepage face, e^{so}, respectively. We note that in (12) we have considered no leakage at the bottom of the aquifer, i.e., $e^s_{\text{bot}} = 0$, and negligible mass transfer between the saturated zone and the reach across the channel bed surface, i.e., $e^{sr} = 0$.

3.3. Unsaturated Zone Momentum Conservation

The conservation of the water phase momentum in the unsaturated zone as derived by *Reggiani et al*. [1998] is

$$(\rho\varepsilon s^u y^u \omega^u)\frac{d}{dt}\mathbf{v}^u - \rho^u \varepsilon y^u s^u \mathbf{g}^u \omega^u = \mathbf{T}^{uA} + \mathbf{T}^{us} + \mathbf{T}^{uc} + \mathbf{T}^u_{wg} + \mathbf{T}^u_{wm}, \tag{13}$$

where $\mathbf{v}^u$ is the average water velocity and $\mathbf{g}^u$ is the gravitational acceleration. The terms on the right-hand side are the various forces acting on the water phase, i.e., the force acting on the mantle surface, $\mathbf{T}^{uA}$ $[FL^{-2}]$, the force exerted on the water table, $\mathbf{T}^{us}$, the force exerted on the unsaturated soil surface, $\mathbf{T}^{uc}$, and the forces exchanged on the water-gas and water-soil interfaces within the porous medium, $\mathbf{T}^u_{wm}$ and $\mathbf{T}^u_{wg}$, respectively.

3.4. Saturated Zone Momentum Conservation

The balance equation for momentum in the saturated zone is

$$(\rho\varepsilon y^s \omega^s)\frac{d}{dt}\mathbf{v}^s - \rho\mathbf{g}^s y^s \varepsilon^s \omega^s = \mathbf{T}^{sA} + \mathbf{T}^{s\ \text{bot}} + \mathbf{T}^{so} + \mathbf{T}^{su} + \mathbf{T}^s_{wm}, \tag{14}$$

where $\mathbf{v}^s$ is the average water velocity in the saturated zone. The terms on the right-hand side are the forces acting on the water in order of appearance: the force acting on the mantle surface, $\mathbf{T}^{sA}$, the force acting on the bottom of the aquifer, $\mathbf{T}^{s\ \text{bot}}$, the force exchanged across the seepage face with the saturated overland flow, $\mathbf{T}^{so}$, the force exchanged on the water table, $\mathbf{T}^{su}$, and the force exerted on the water phase due to contact with the soil matrix, $\mathbf{T}^s_{wm}$. The momentum conservation laws (13) and (14) are vectorial equations, which need to be projected along the axes of the reference system in Figure 1 by scalar multiplication with the unit vectors $\mathbf{e}_x$, $\mathbf{e}_y$, and $\mathbf{e}_z$, respectively. The results of this procedure are presented in section 3.5.

3.5. Projection of the Momentum Balance Equations

The momentum balance equations (13) and (14) reported above, govern the three-dimensional flow within the REW. These equations need to be projected along the axes of the reference system in Figure 1. In order to simplify the problem significantly, we first state a series of assumptions on the geometry of the REW:

1. The bottom boundary of the REW is near-flat, such that the horizontal force acting on it is negligible:

$$\mathbf{T}^{s\ \text{bot}} \cdot \mathbf{e}_x = \mathbf{T}^{s\ \text{bot}} \cdot \mathbf{e}_y \approx 0. \tag{15}$$

2. The slope of the land surface within the REW boundaries is overall small such that the horizontal force acting on the water in the unsaturated and the saturated zones across the land surface can be considered negligible:

$$\mathbf{T}^{uc} \cdot \mathbf{e}_x = \mathbf{T}^{uc} \cdot \mathbf{e}_y = \mathbf{T}^{so} \cdot \mathbf{e}_x = \mathbf{T}^{so} \cdot \mathbf{e}_y \approx 0. \tag{16}$$

3. In the absence of regional groundwater flow (as we have an isolated REW) the resultant of the horizontal forces acting on the closed prismatic mantle surface surrounding the REW laterally are negligible:

$$\mathbf{T}^{uA} \cdot \mathbf{e}_x = \mathbf{T}^{uA} \cdot \mathbf{e}_y = \mathbf{T}^{sA} \cdot \mathbf{e}_x = \mathbf{T}^{sA} \cdot \mathbf{e}_y \approx 0. \quad (17)$$

4. The water table is near-horizontal:

$$\mathbf{T}^{us} \cdot \mathbf{e}_x = \mathbf{T}^{us} \cdot \mathbf{e}_y \approx 0. \quad (18)$$

5. The average vertical flow in the saturated aquifer is negligible:

$$\mathbf{v}^s \cdot \mathbf{e}_z \approx 0. \quad (19)$$

In view of assumptions 1–4 and neglecting inertial forces, the horizontal components of (13) and (14) reduce to

$$(\mathbf{T}^u_{wg} + \mathbf{T}^u_{wm}) \cdot \mathbf{e}_x = (\mathbf{T}^u_{wg} + \mathbf{T}^u_{wg}) \cdot \mathbf{e}_y = 0 \quad (20)$$

$$\mathbf{T}^s_{wm} \cdot \mathbf{e}_x = \mathbf{T}^s_{wm} \cdot \mathbf{e}_y = 0. \quad (21)$$

Equations (20) and (21) simply imply that no net horizontal flow occurs in the two subsurface zones. The only nonzero flow occurs along the vertical direction in the unsaturated zone. Consequently, we project the conservation equation of momentum along $\mathbf{e}_z$. We note that the z coordinate is positive upward, such that $\mathbf{g}^u \cdot \mathbf{e}_z = -g$. The inertial term in (13) is neglected, a common assumption for slow flows, so that the following balance of forces along z is obtained:

$$\rho g \varepsilon y^u s^u \omega^u = T^{us}_z + T^{uc}_z + T^u_{wg,z} + T^u_{wm,z}. \quad (22)$$

Owing to assumption 5, the vertical component of (14) reduces simply to a static balance of forces. As shown by *Reggiani et al*. [1999a], the average pressure for the aquifer can be calculated in terms of the difference in gravitational potential evaluated between the water table, at an average elevation $y^s + z^s$ above the datum, and at the center of mass of the unsaturated zone, situated at an elevation $y^s/2 + z^s$ above the datum (for reference, see Figure 3):

$$p^s = \rho g[y^s + z^s - \tfrac{1}{2}y^s - z^s] = \tfrac{1}{2}\rho g y^s. \quad (23)$$

4. Closure of the Equations

The balance laws presented in section 3 need to be supplemented with constitutive relationships to close the unknown mass fluxes and force exchanges which appear on the right-hand side of the four conservation equations: (11), (12), (13), and (14). The closure of the equations has been carried out rigorously by *Reggiani et al*. [1999a] for an entire watershed discretized into a finite number of REWs, each consisting of five different subregions. For this purpose the *Coleman and Noll* [1963] procedure, based on the exploitation of the second law of thermodynamics, has been employed to develop constitutive relationships in a systematic fashion. For reasons of brevity we omit the description of the procedure, and here we present only the final results.

Furthermore, we have not yet pursued a rigorous study of the bare soil evaporation and plant transpiration components of the water balance. This is because they would require the inclusion of the atmospheric boundary layer into the REW as an additional averaging region and the consideration of the mobility of the air-vapor mixture within and above the soil pores. For these reasons we have excluded a separate treatment of plant transpiration and, instead, have decided to include a rather simplistic parameterization of evapotranspiration (combination of evaporation and transpiration) as a preliminary step to complete the hydrologic cycle at the REW scale. A more rigorous representation of evapotranspiration is an urgent issue vis à vis the theoretical development which is being pursued here and is left for further research.

The mass fluxes e^u_{wg}, e^{us}, e^{uc}, and e^{os}, expressed on a per-unit-area basis and accounting for evapotranspiration, groundwater recharge or capillary rise, infiltration, and seepage, must satisfy the continuity conditions (i.e., jump conditions) across both internal and external boundaries of the REW, such as the water table, the seepage face, or the unsaturated land surface. This is equivalent to stating that the exchange from the region j (e.g., unsaturated zone) toward the region k (e.g., saturated zone) has to equal the exchange in the opposite direction:

$$e^{jk} + e^{kj} = 0. \quad (24)$$

As shown by *Reggiani et al*. [1999a], in general, these mass exchange terms are functions of the mean values of the velocities on both sides of the boundary and the difference in hydraulic potentials $(p + \zeta\rho g)$. Ideally, such functions have to be determined from field observations (or, in some cases, from detailed numerical modeling). However, in physics and for practical applications, as a first approximation, a linear dependence is commonly assumed. Thus we propose that

$$e^{jk} = \mathscr{A}^{jk}(p^k + \zeta^k\rho g - p^j - \zeta^j\rho g) - \mathscr{B}^{jk}\tfrac{1}{2}(\mathbf{v}^j + \mathbf{v}^k) \cdot \mathbf{A}^{jk}, \quad (25)$$

where the coefficients $\mathscr{A}^{jk}$ and $\mathscr{B}^{jk}$ are functions of the system variables, while $\mathbf{A}^{jk}$ is an areal vector, defined as

$$\mathbf{A}^{jk} = \frac{1}{\Sigma} \int_{A^{jk}} \mathbf{n}^{jk}\, dA\, d\tau. \quad (26)$$

The area A^{jk} forms the fluid part of the boundary between the subregions j and k (e.g., the water table A^{us} or the land surface A^{cu}) and unit vector $\mathbf{n}^{jk}$ is normal to A^{jk}, pointing outward. This is equivalent to stating that the mass exchange term is given by a linear superimposition of a component related to the mean velocity and a component attributable to pressure head difference. We propose a linearization of the mass flux e^{jk} in terms of velocity or pressure head differences by imposing either $\mathscr{A}^{jk}$ or $\mathscr{B}^{jk}$ to be zero. This is done to simplify the final expressions of the parameterized balance equations. We observe that if such a linearization should prove inadequate for the description of the system, a full parameterization, with both $\mathscr{A}^{jk}$ and $\mathscr{B}^{jk}$ being nonzero, can be employed. We do not exclude that the above linear parameterization of the mass exchange term may be replaced in the future by a more complex expression by taking into account higher-order effects. This is part of an iterative procedure, aimed at improving the constitutive relationships, as more insights are gained through field, laboratory, and numerical experiments.

4.1. Infiltration (e^{uc})

The flux term expressing the infiltration of water across the soil surface into the unsaturated zone is linearized in terms of the difference in hydraulic potentials between the (infiltration excess) overland flow zone and the unsaturated zone. Under potential conditions, i.e., when the soil surface is saturated, the average pressure in the infiltration excess zone is essentially equal to the (zero) atmospheric pressure. The average water

pressure p^u in the pores of the unsaturated zone is assigned through the spatial average capillary pressure (7):

$$p_{\text{cap}} = p_{\text{atm}} - p^u = -p^u. \tag{27}$$

Therefore the rate of infiltration of the soil surface is given by

$$e^{uc} = -e^{cu} = \mathcal{A}^{uc}(\zeta^c \rho g + p_{\text{cap}} - \zeta^u \rho g), \tag{28}$$

where ζ^c and ζ^u are given by (5) and (3), respectively. The term e^{uc} acts as a source term for the unsaturated zone and as a sink term for the concentrated overland flow (infiltration excess flow) subregion. Consequently, the function $\mathcal{A}^{uc}$ needs to be always positive. We define $\mathcal{A}^{uc}$ as

$$\mathcal{A}^{uc} = \frac{K_{\text{sat}} \omega^u}{g \Lambda_u} \tag{29}$$

where K_{sat} $[L T^{-1}]$ is the saturated hydraulic conductivity and Λ_u $[L]$ is a typical length scale of the problem under study. We chose Λ to be proportional to the thickness of the unsaturated zone y^u:

$$\Lambda_u = s^u y^u. \tag{30}$$

This length scale represents an approximation for the depth of a wetting front in a piston-type model of infiltration. Equation (28) resembles traditional infiltration capacity equations such as the Green-Ampt equation. We note that in the case of a rainfall intensity i, which is lower than the infiltration capacity described by (28), all rainfall infiltrates, and e^{uc} is climate controlled and is equal to $e^{uc} = \rho i \omega^u$. Consequently, the expression

$$e^{uc} = \min \left[\rho i \omega^u, \frac{K_{\text{sat}} \omega^u}{g \Lambda_u} (\zeta^c \rho g + p_{\text{cap}} - \zeta^u \rho g) \right] \tag{31}$$

is used to estimate the actual infiltration at every time step. Nevertheless, (31) has ignored the spatial variability of rainfall, the soils, or the presence of macropores and thus has to be generalized appropriately. This is perfectly feasible, provided that adequate catchment-scale field measurements can be performed or published experimental data can be exploited to guide and to validate such generalized equations.

4.2. Recharge to Water Table Capillary Rise (e^{us})

For the closure of the mass flux across the water table we propose a linearization in terms of the vertical velocity in the unsaturated zone, v^u. Note that v^u is considered positive upward. The vertical component of the area vector $\mathbf{A}^{us}$ defined in (26) can be approximated as $\mathbf{A}^{us} \cdot \mathbf{e}_z = \omega^u \varepsilon$. Therefore the mass flux across the water table becomes

$$e^{us} = -e^{su} = \rho v^u \omega^u \varepsilon, \tag{32}$$

where we recall that we have assumed no vertical flow in the saturated zone (see assumption 5 in section 3). In this manner the mass exchange term describes recharging of the saturated zone (water table) when v^u is negative and capillary rise from the water table when v^u is positive. The parameter $\mathcal{B}^{us}$ is required to be always positive as a velocity is considered positive when directed upward.

4.3. Seepage Outflow (e^{so})

The seepage outflow from the saturated zone can eventuate even when the average flow velocity within this aquifer is zero. As indicated by equation (25), as a first approximation, we assume a linear dependence of the seepage outflow on the hydraulic potential difference between the aquifer and the seepage face:

$$e^{so} = -e^{os} = \mathcal{A}^{so}(\zeta^o \rho g - p^s - \zeta^s \rho g), \tag{33}$$

where the average pressure on the seepage face is assumed to be atmospheric ($p^o = 0$), while ζ^s and ζ^o are given by (2) and (4), respectively. The average pressure in the aquifer p^s, to be used in (33), is calculated through (23). For similar physical reasons as in the above cases the linearization parameter $\mathcal{A}^{so}$ must be a positive function and is postulated as

$$\mathcal{A}^{so} = \frac{K_{\text{sat}} \omega^o}{\cos(\gamma^o) g \Lambda_s}. \tag{34}$$

The parameter K_{sat} $[L T^{-1}]$ is the average saturated hydraulic conductivity and Λ_s $[L]$ is a typical length scale, which depends on the lateral dimension of the system (e.g., length of the hillslopes) and has to be determined from either field studies or with the aid of detailed numerical models based on small-scale balance equations (e.g., Richards equation). The length scale Λ_s is a measure of the distance over which the difference in hydraulic potentials between the saturated zone and the seepage face is dissipated. Therefore Λ_s constitutes a radius of influence of the seepage face on the flow field within the aquifer. It is expected to be comparable with the length of the hillslope and to vary between 10^1 and 10^3 m. For the present application we have arbitrarily set Λ_s to 10 m, regardless of the length of the hillslope. We note that Λ_s can be envisaged as a REW-average surrogate for the hillslope length scale, a parameter commonly employed in traditional hillslope models. The presented expression constitutes only a first estimate, which requires further investigation and needs to be underpinned by field and laboratory experiments. These studies can educate us on how best to parameterize (28), (32), and (33).

The average slope angle γ^o of the seepage faces can be a function of the size of the seepage face, expressed by ω^o, and can vary as the saturated areas expand or contract, encompassing generally steeper segments of the hillslope. In this application we assume γ^o to be a constant value:

$$\cos(\gamma^o) = S^o / \Sigma^o \approx \text{const}. \tag{35}$$

4.4. Evapotranspiration

To represent evapotranspiration from the unsaturated land surface areas, we propose a rather simple constitutive relationship. It is based on the assumption that actual evapotranspiration is linearly proportional to the potential rate of evapotranspiration e_p:

$$e^u_{wg} = -e^u_{gw} = -e_p \rho \omega^u s^u, \tag{36}$$

where the proportionality constant is given by the product of the unsaturated land surface fraction and the average saturation of the unsaturated zone. As the saturation s^u approaches the value of unity, actual evapotranspiration approaches its maximum (potential) rate, whereas with decreasing soil saturation the evapotranspiration rate is assumed to decrease proportionally, reaching zero for $s^u = 0$.

To complete the water balance, the evaporation $e^{o\ \text{top}}$ from the seepage face needs to be accounted for. In this case we assume that water evaporates from the seepage faces at the potential rate $\rho e_p \omega^o$ during interstorm periods if the supply of

moisture through the seepage outflow e^{so} is higher than the absorption through the evaporation; otherwise, the evaporation is limited by the amount of moisture supplied by e^{so}. Therefore the evaporation from the saturated areas is given by

$$e^{o\ \mathrm{top}} = \min\,[e^{so},\ \rho e_p \omega^o]. \tag{37}$$

If the supply of moisture exceeds the amount evaporated at the potential rate, the remaining water becomes surface runoff.

We must emphasize that these are temporary, and expedient, assumptions. A rigorous analysis of evapotranspiration requires inclusion of considerable additional processes and associated physics. These must include (1) movement of liquid soil moisture from deeper levels to the soil surface or to plant roots; (2) phase change from the liquid phase to the gaseous phase, both within the soil pores and within the stomata of plant leaves; and (3) exchange of such moisture with the atmosphere. As a first step, these have been ignored here in favor of the simplistic approach presented above.

4.5. Momentum Exchange Terms for the Unsaturated Zone

As shown in section 3, on the basis of assumptions 1–4 the horizontal momentum balance is deemed to be trivially zero for the unsaturated zone and saturated zones. The only direction along which forces are not balanced is the vertical. Along the vertical, the total force acting on the water phase is the sum of two components: (1) an equilibrium part attributable to the pressure and (2) a nonequilibrium part, which becomes zero at equilibrium (i.e., in the absence of flow). Under nonequilibrium conditions (nonzero velocity), viscous forces appear next to the pressure force caused by the motion of the fluid. As shown by *Reggiani et al*. [1999a], we can write the sum of vertical forces acting on the water phase within the unsaturated zone as

$$T_z^{us} + T_z^{uc} + T_z^{us} + T_{wg,z}^{u} + T_{wm,z}^{u} = T_z^{us}|_e + T^{uc}|_e + T_z^{us}|_e + T_{wg,z}^{u}|_e + T_{wm,z}^{u}|_e + \bar{\tau}_z^{u}. \tag{38}$$

First, we observe that the equilibrium force exerted on the water table, $T_z^{us}|_e$, is zero due to the atmospheric (zero) pressure on the phreatic surface and that the forces $T_{wg,z}^{u}|_e$ and $T_{wm,z}^{u}|_e$ exerted by the gas and the soil matrix on the water phase in the soil pores are zero for symmetry reasons. With respect to the force acting on the water phase at the land surface, $T_z^{uc}|_e$, *Reggiani et al*. [1999a] found the following expression for the equilibrium part of the acting forces:

$$T_z^{u}|_e = T_z^{uc}|_e = \rho g[-p^u + \tfrac{1}{2} y^s], \tag{39}$$

where p^u can be obtained through the Brooks and Corey formula (7). Next, the nonequilibrium part can be expanded as a first-order function of velocity, so that it yields an exchange term equivalent to Darcy's law. This procedure is based on a first-order Taylor series expansion, which is valid under slow flow conditions:

$$\bar{\tau}_z^{u} = -R^u v^u \tag{40}$$

and should be generalized with higher-order expansions when the slow flow assumption is no longer appropriate. For homogeneous, isotropic soils the resistivity R^u $[FTL^{-3}]$ is a function of the average saturation of the soils and the geometry of the unsaturated zone, expressed in terms of the average depth y^u, the area fraction ω^u, and the porosity ε:

$$R^u = [K(s^u)]^{-1} \varepsilon \rho g y^u \omega^u, \tag{41}$$

where $K(s^u)$ is given by (8). When substituted into (11), (12), and (22), expressions (28), (32), (33), (36), (39), and (40) will lead to the parameterized forms of the balance equations. These are reported in Appendix A. In Appendix B we derive a constitutive relationship, based on geometrical considerations, which is needed to make the equation system in Appendix A determinate.

5. Dimensionless Equations

The parameterized balance equations and respective closure schemes for mass and momentum exchange terms are reported in Appendix A and in section 4. These equations can be cast into nondimensional form. This procedure allows us to study the system in a general manner, by analyzing the sensitivity of water balance to changes in topography (flatness or steepness), soil properties, and atmospheric forcing. To pursue such a similarity analysis of the equations, we need to introduce three families of relevant dimensionless quantities.

First, we define the relevant timescales. We first define a percolation (soil) timescale t_s, defined as $t_s = \varepsilon Z/K_{\mathrm{sat}}$, the ratio of porous fraction of the total soil thickness over saturated hydraulic conductivity. The simulation time t can then be nondimensionalized with respect to t_s as follows: $t^* = t/t_s$. A further two timescales are the storm duration t_r and the interstorm period t_b. The sum $t_a = t_r + t_b$ is the total length of one climatic cycle and may be made dimensionless by dividing through t_s, thus giving $t_a^* = t_r^* + t_b^*$.

Second, we introduce the following dimensionless numbers characterizing topographic elevation, climate, and soil: $L^* = \psi_b/Z$, the soil index, is the ratio of bubbling pressure head over total average soil thickness; $e_p^* = e_p/K_{\mathrm{sat}}$ is the nondimensional potential rate of evapotranspiration; $p^* = i/K_{\mathrm{sat}}$ is the nondimensional rainfall intensity; $Z^* = (z^r - z^s)/Z$ is a geometric parameter labeled flatness index since an increase in Z^* corresponds to increasing flatness of the watershed; $R^* = E_{P_A}/P_A$ is the ratio of total annual potential evapotranspiration over total annual precipitation, called the dryness index; and $T^* = t_b/t_r$ is the ratio of interstorm period over storm duration, here called the storminess index, because increasing T^* corresponds to shorter-duration storms. In addition, we also provide dimensionless forms for the length scales Λ_u and Λ_s, defined as $\Lambda_u^* = \Lambda_u/Z$ and $\Lambda_s^* = \Lambda_s/Z$, respectively.

Third, we introduce the following additional symbols and dimensionless quantities: $s^* = s^u$ is the spatially averaged saturation of the unsaturated zone, $\omega^* = \omega^o$ is the saturated area fraction of the REW. Both quantities are already dimensionless in the way they have been defined in the balance equations in section 3. The quantity $y^* = y^s/Z$ is the dimensionless form of the depth of the saturated zone, while $v^* = v^u \varepsilon/K_{\mathrm{sat}}$ is the dimensionless unsaturated zone velocity.

The ensemble of dimensionless parameters defined above is summarized in Table 3. The similarity analysis of the governing equations requires a number of additional preliminary similarity considerations: First, we observe that the area fraction ω^u of the unsaturated zone can be expressed in terms of the new symbol ω^* replacing ω^o:

$$\omega^u = (1 - \omega^o) = (1 - \omega^*). \tag{42}$$

Second, from (B1) the average thickness of the unsaturated zone can be expressed in terms of the dimensionless quantity y^*:

Table 3. Summary of Dimensionless Quantities

	Quantity	Definition	Description
1[a]	t_s	$\varepsilon Z/K_{\text{sat}}$	percolation timescale
	t^*	t/t_s	simulation time
	t_r^*	t_r/t_s	storm duration
	t_b^*	t_b/t_s	interstorm period
	t_a^*	t_a/t_s	climatic period
2[a]	L^*	ψ_b/Z	soil index
	Z^*	$(z^r - z^s)/Z$	flatness index
	R^*	E_{P_A}/P_A	dryness index
	T^*	t_b/t_r	storminess index
	e_p^*	e_p/K_{sat}	potential evapotranspiration
	p^*	i/K_{sat}	rainfall intensity
	Λ_u^*	Λ_u/Z	infiltration length scale Λ_u
	Λ_s^*	Λ_s/Z	surrogate hillslope length scale Λ_s
3[a]	s^*	s^u	average saturation
	ω^*	ω^o	saturation area fraction
	y^*	y^s/Z	aquifer depth
	v^*	$\varepsilon v^u/K_{\text{sat}}$	percolation velocity

[a]See section 5 for discussion of the three families of relevant dimensionless quantities.

$$y^u/Z = \frac{(1 - y^*)}{(1 - \omega^*)}. \tag{43}$$

With these definitions and observations it is now possible to perform a dimensional (similarity) analysis on the balance equations (A1), (A2), and (A3) given in Appendix A.

5.1. Balance of Mass for the Unsaturated Zone

We recast (A1) into a nondimensional form with the aid of the above defined quantities, obtaining

$$\frac{d}{dt^*}[s^*(1 - y^*)] = \min\left\{p^*(1 - \omega^*), \frac{1}{\Lambda_u^*}\left[\tfrac{1}{2}(1 - y^*) - (1 - \omega^*)L^*(s^*)^{-1/\mu}\right]\right\}\delta[0, t_r^*] + (1 - \omega^*)v^* - e_p^* s^*(1 - \omega^*)\delta[t_r^*, t_a^*], \tag{44}$$

where the term on the left-hand side is storage, the first term on the right-hand side is infiltration, the second term is percolation/capillary rise, and the last term is evaporation. The function $\delta[a, b]$ is equal to 1 when t^* falls between the values a and b shown within the brackets and is zero otherwise. Equation (44) will be employed to evaluate the average saturation s^*.

5.2. Balance of Momentum for the Unsaturated Zone

The conservation of momentum is derived from the REW-scale unsaturated zone Darcy's law (A2) derived in Appendix A:

$$-(1 - y^*) + \left[\tfrac{1}{2}(1 - y^*) - (1 - \omega^*)L^*(s^*)^{-1/\mu}\right] = -\left[\varepsilon(s^*)^{(1+\lambda)}\right]^{-1}(1 - y^*)v^*, \tag{45}$$

where the first term on the left-hand side is gravity, the second term is the force acting on the water phase across the land surface, and the right-hand side term is the resistance acting on the water within the pores. This algebraic equation will be utilized to calculate the average dimensionless velocity v^* within the unsaturated zone.

5.3. Balance of Mass for the Saturated Zone

The mass balance for the saturated zone is obtained after substituting the dimensionless variables into the balance equation (A3):

$$\frac{d}{dt^*}y^* = -(1 - \omega^*)v^* - \frac{\omega^*}{\cos(\gamma^o)\Lambda_s^*}\frac{1}{2}(y^* - Z^*), \tag{46}$$

where the left-hand side is storage, while the right-hand side terms represent percolation/capillary rise and outflow across the seepage faces, respectively. Equation (46) yields the average unsaturated zone depth y^*. An additional relationship, relating ω^* to y^* and therefore eliminating one unknown, is presented in Appendix B. This relationships needs also to be cast into dimensionless form:

$$\omega^* = \omega^*(y^*) = \frac{(y^* - Z^*)}{(1 - Z^*)}. \tag{47}$$

Equations (44)–(47) compose a set of nonlinear coupled equations in terms of s^*, y^*, ω^*, and v^*. The numerical solution of the system, made determinate with the inclusion of (47), and the discussion of the results will be addressed in section 6.

6. Numerical Application

Employing the dimensionless balance equations presented in section 5, we undertake a series of simulations of the fluxes of water through single REWs and exchanges with the atmosphere. These simulations are carried out for various combinations of geometries (steepness of topography), climate, and soil types. For the type of REW under study the governing equations consist of the two nonlinear ordinary differential equations (44) and (46) for y^* and s^*, governing the balance of mass for the unsaturated and saturated zones and the algebraic equation (45) for the estimation of the vertical flow velocity across the unsaturated zone. All three equations are fully coupled between themselves. Equation (47) is needed to complete the system.

We solve this system of ordinary differential equations (ODEs) by adopting a numerical algorithm presented by *Press et al.* [1992, pp. 714–722]. The algorithm is based on the Runge-Kutta integration method, supplemented with adaptive step-size control. This control procedure allows one to monitor the local truncation error at every time step during the computation.

The simulations are run over a fixed time period t_a^*, which is separated into a storm duration t_r^*, and a subsequent interstorm period t_b^* (see Figure 4). Initial conditions are unknown for each of these ODEs, and therefore initial values for the variables need to be imposed at the beginning of the simulations. Initial conditions are needed for each of these ODEs. Thus the saturation s^* is set to an initial value s_0^*, the dimensionless water table depth y^* to a value y_0^*.

Starting with these initial values, the responses of the watershed and its subregions are simulated by solving the above ODEs over the time period t_a^* representing a complete storm and interstorm period, computing the values of s^*, v^*, and y^* at every time step along the way. At the end of one climatic cycle the values of saturation s_0^* and water table depth y_0^* at the beginning ($t^* = 0$) are compared with the corresponding values at the end of once climatic cycle ($t^* = t_a^*$). If they differ by a significant margin, then the arithmetic average between above two values, initial and final, is taken to be the new initial

value, and the simulations are repeated. For example, the new initial values for the $i + 1$st iteration are estimated as

$$s^*_{0,i+1} = (s^*_{0,i} + s^*_{t_a^*,i})/2$$
$$y^*_{0,i+1} = (y^*_{0,i} + y^*_{t_a^*,i})/2. \quad (48)$$

After a number of iterations we finally arrive at sufficiently close initial and final values for water table depth and saturation, which can be taken to be equilibrium water table position and equilibrium saturation, respectively. These are indeed consistent with equilibrium in an *Eagleson* [1978a, c] sense; that is, they are dynamic equilibrium values corresponding to the given topography (steepness), soil type, and atmospheric forcing. The methodology adopted and the resulting equilibrium values are perfectly appropriate in this case considering the type of deterministic and repetitive climate cycle assumed here. They will not be valid if one has to deal with random climatic inputs, as in the work by *Eagleson* [1978a].

7. Investigation of the Controls on the REW Water Balance

In this section we investigate the physical controls on long-term water balance using the numerical model described in section 6. Note that the model solves the set of dimensionless, watershed-scale mass and momentum balance equations for the two subsurface zones (unsaturated and saturated zones) within a single REW. We investigate how spatiotemporal averages of the soil saturation (within the unsaturated zone) and of the water table depth are governed by climatic factors, soil properties, and topography (i.e., flatness of the land surface). The climatic factors considered are the dryness index $R^* = E_{P_A}/P_A$ and the storminess index $T^* = t_b/t_r$. For soils we consider three generic soil types, with decreasing permeability and increasing water retention capacity: sands, sandy loams, and silty loams. For topography we used the flatness index $Z^* = (z^r - z^s)/Z$.

Overall, we carried out three sets of simulations. In case 1 we investigate the effect of topography by varying the flatness index Z^*, while keeping constant the dryness index R^* and the storminess index T^*. In case 2 we investigate the effect of the climatic dryness or aridity by varying the dryness index R^*, while keeping constant the flatness Z^* and storminess T^* indices. Finally, in case 3 we investigate the effect of storminess of rainfall by varying T^*, while keeping constant the dryness index R^* and the flatness Z^*. In all three cases the simulations are repeated for the soil types, sand, sandy loam, and silty loam, whose physical characteristics have been summarized in Table 1. For the quantities required to characterize geometry and climate, the specific values indicated in Table 4 have been selected for the numerical simulations.

Table 4. Numerical Values for the Model Parameters

Parameter	Selected Value
t_a	107 hours
t_r	10–50 hours
Z	8 m
$z^r - z^s$	3–7 m
i	0.74–3.0 mmh^{-1}
e_p	8.95 mm d^{-1}
Λ^s	10 m

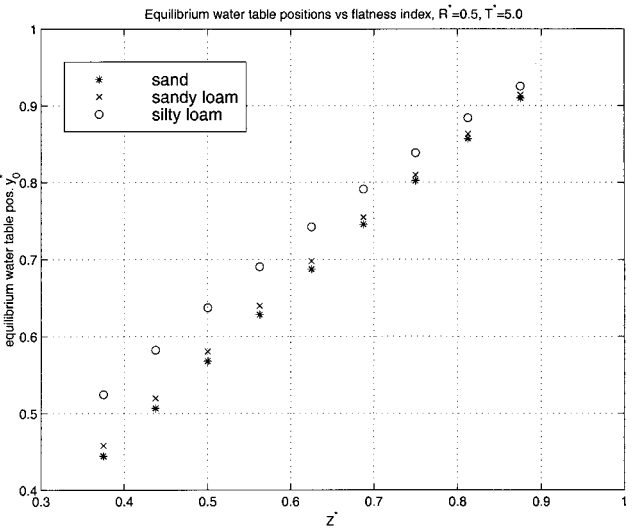

Figure 5a. Effect of flatness on water table position.

The results are interpreted in relation to both physical intuition and governing equations. This discussion is presented in sections 7.1–7.3.

7.1. Case 1: Topography: Flatness Index and Soils

A series of simulations have been performed, where different topographies in terms of the dimensionless variable Z^*, in the range $0.375 \leq Z^* \leq 0.875$, were investigated. The climate is assumed to be humid, characterized by a dryness index $R^* = 0.5$, i.e., the total annual evapotranspiration E_{P_A} amounts to half of the total annual precipitation P_A. The storminess index T^*, the ratio between the interstorm period t_b and the storm duration t_r, is kept at the constant value 5.0. The simulations were carried out for three distinct soil types: sand, sandy loam, and silty loam. The dimensionless soil property L^*, which is the ratio of the bubbling pressure head ψ_b and the total average depth of the soil Z, remains constant for a given soil but differs between soil types. The results of the simulations are reported in Figures 5a–5e.

Figures 5a and 5b show the variations of the equilibrium

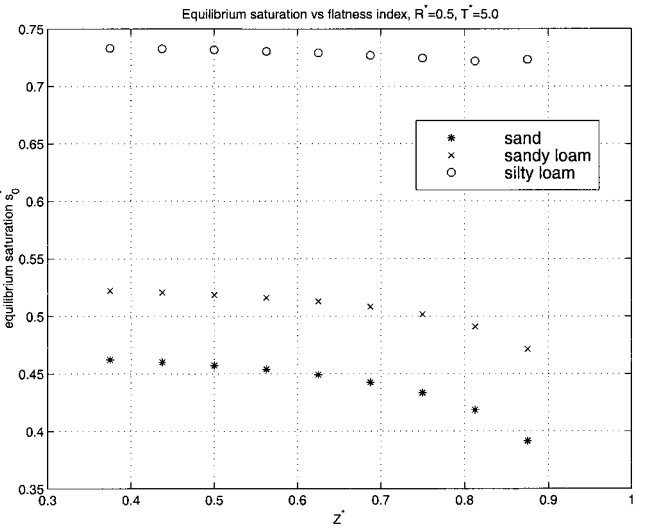

Figure 5b. Effect of flatness on level of saturation.

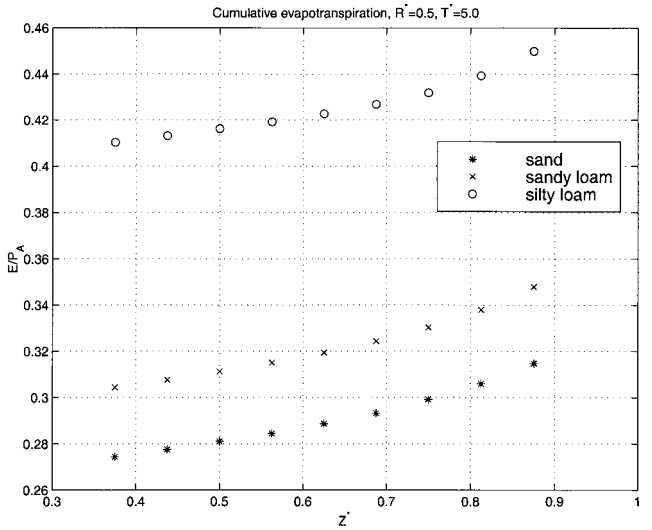

Figure 5c. Effect of flatness on cumulative annual evapotranspiration.

water table position y^* and equilibrium saturation s^* as functions of the flatness index Z^* for the three different soil types. We observe that decreasing permeability of the soil (changing from sand to sandy loam to silty loam) and increasing flatness of the watershed (Z^* approaching unity) combine together to cause slower drainage of the watershed. This leads to higher equilibrium water table elevations (i.e., water table reaching closer to the soil surface), as seen in Figure 5a. Yet while the water table rises as the watershed becomes flatter, the equilibrium soil saturation actually decreases, as seen in Figure 5b, especially for more permeable soils, which is somewhat counterintuitive. However, a first-order analysis of the water balance for constant climate (i.e., constant R^*) suggests that s^* does indeed decrease nonlinearly with increasing y^*. Part of the explanation for this is that the storage of water in the unsaturated zone is the product of s^* and y^*, while the evapotranspiration and deep percolation are proportional to s^*, not to the product of s^* and y^*. Flatter and less permeable watersheds establish generally higher equilibrium water table positions and higher saturation values.

Figure 5c shows the total cumulative evapotranspiration over the simulation period (one cycle only). It is evident that flatter watersheds, since they exhibit generally higher saturation values over much of the climatic cycle, yield larger values of evapotranspiration. Similarly, Figure 5d presents cumulative volumes of subsurface runoff discharging across the seepage face. The seepage outflow is driven by the difference in hydraulic potentials between aquifer and seepage face and by the permeability of the soil, both of which are reflected in the results. It can be seen that more permeable soils (e.g., sand) yield higher overall subsurface runoff volumes than their less permeable counterparts (e.g., silty loam).

For silty loam in flat watersheds the rate at which the seepage face delivers water is smaller than the amount of water evaporated on the surface, and therefore V_{ss}/P_A is zero in these cases, as evident from Figure 5d. Similarly, steeper watersheds (i.e., lower Z^*) produce larger subsurface runoff volumes due to the higher hydraulic potential differences between the aquifer and the seepage face. Overall, the combination of more permeable soils and steeper hillslopes leads to a well-drained landscape, yielding higher subsurface runoff contributions.

Finally, we combine the above results and present, in Figure 5e, the effect of the flatness index Z^* on the overall water balance partitioning over the climatic cycle. This is equivalent, under the climatic forcing assumptions of this study, to the annual water balance partitioning. Figure 5e shows in one plot, on a scale of 0 to 1, the proportions of total precipitation which go into evapotranspiration, subsurface runoff, and surface runoff (combination of direct precipitation onto the seepage faces and infiltration excess runoff). We observe that with increasing Z^* (i.e., flatter watersheds) more water is running off from the soil surface as overland flow or is evaporated, while less water is running off as subsurface flow. This trend is accentuated further for less permeable soils.

7.2. Case 2: Climate: Dryness Index

In this case we fixed the flatness index of the REW to the moderate value of $Z^* = 0.5$ and the value of the storminess index to $T^* = 5.0$. The value of the dryness index was then changed gradually from a value of $R^* = 0.5$, corresponding to a humid climate, to a value of $R^* = 2$, typical of semiarid climates. The simulations were carried out for three distinct soil types: sand, sandy loam, and silty loam, whose physical characteristics are summarized in Table 1. The results are presented in Figures 6a–6c.

Figures 6a and 6b show the variation of the equilibrium water table position y^* and the equilibrium saturation s^* with the dryness index R^*. Both quantities decrease with increasing dryness (or aridity) for all three soils. This indicates that as the climate dries, the water table becomes deeper and the soil gets drier, both of which are intuitively obvious. Once again, both y^* and s^* are higher for less permeable, or poorly drained, soils.

Figure 6c presents the partitioning of total (annual) rainfall into evapotranspiration, subsurface runoff, and surface runoff for the three soil types. We observe that while evapotranspiration increases with increasing dryness index, there is a corresponding decrease of runoff (both surface and subsurface). We also note that similar to the results obtained in case 1, both the evapotranspiration and the surface runoff components are smaller for more permeable soils such as sands (i.e., smaller equilibrium moisture content), while subsurface runoff tends to be higher. In this case, we will not report separate results for

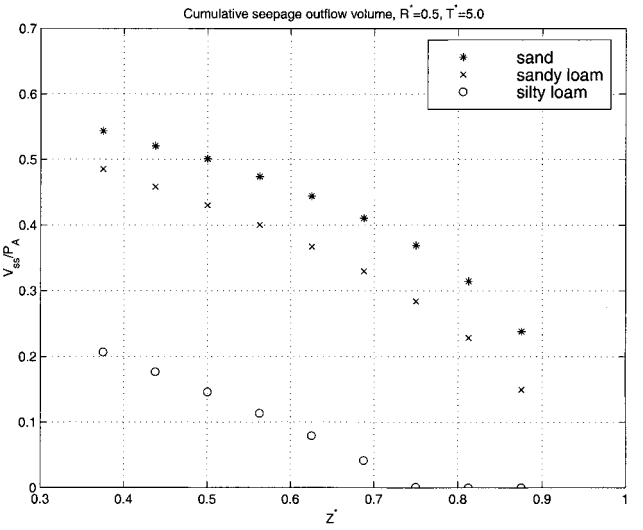

Figure 5d. Effect of flatness on cumulative annual subsurface runoff.

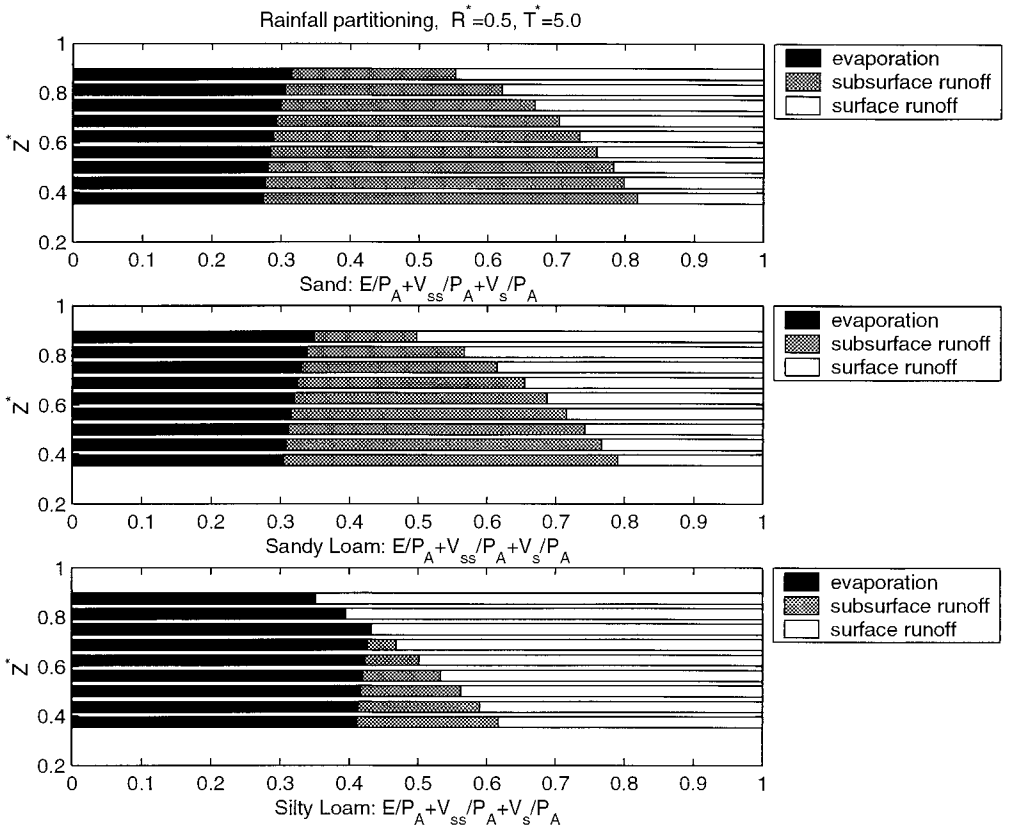

Figure 5e. Effect of flatness on the annual water balance partitioning.

subsurface runoff and evapotranspiration as functions of R^*, as these can be clearly seen in Figure 6c. Surface runoff, including direct precipitation onto the saturated areas and infiltration excess flow, is generally higher for humid catchments and/or in less permeable soils. This is because (1) the infiltration capacity is very much smaller in less permeable soils and (2) the saturated areas are larger in humid catchments and/or in less permeable soils due to the generally higher equilibrium water tables in both situations.

7.3. Case 3: Climate: Storminess Index

The third series of simulations have been carried out by fixing the dryness index to a value of $R^* = 0.5$ and the flatness index to a value of $Z^* = 0.5$ and changing only the storminess index, between $1.16 \leq T^* \leq 10$. Low T^* values correspond to short pulses of high-intensity rainfall, while high T^* values correspond to long-duration, light-intensity rain. The total rainfall partitioning with changing storminess T^* is reported in

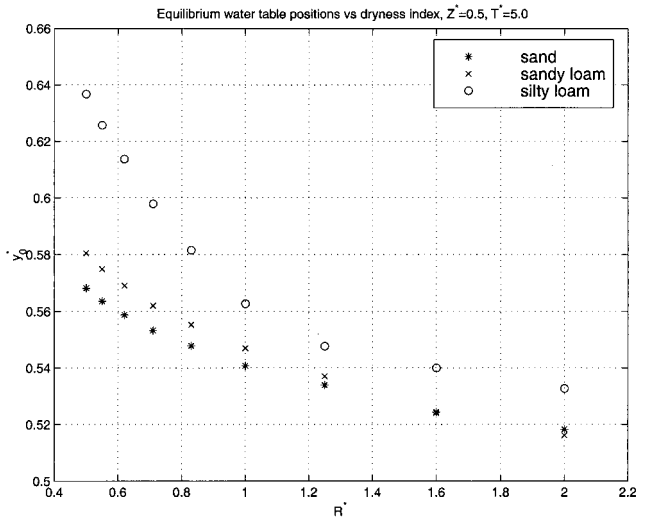

Figure 6a. Effect of climatic dryness on water table position.

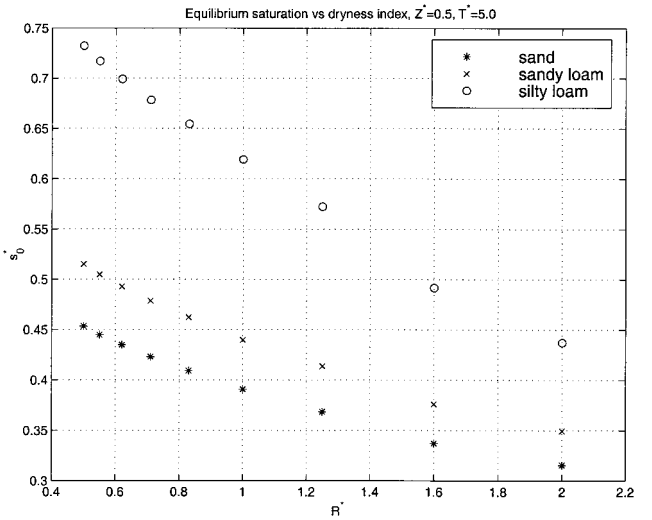

Figure 6b. Effect of climatic dryness on level of saturation.

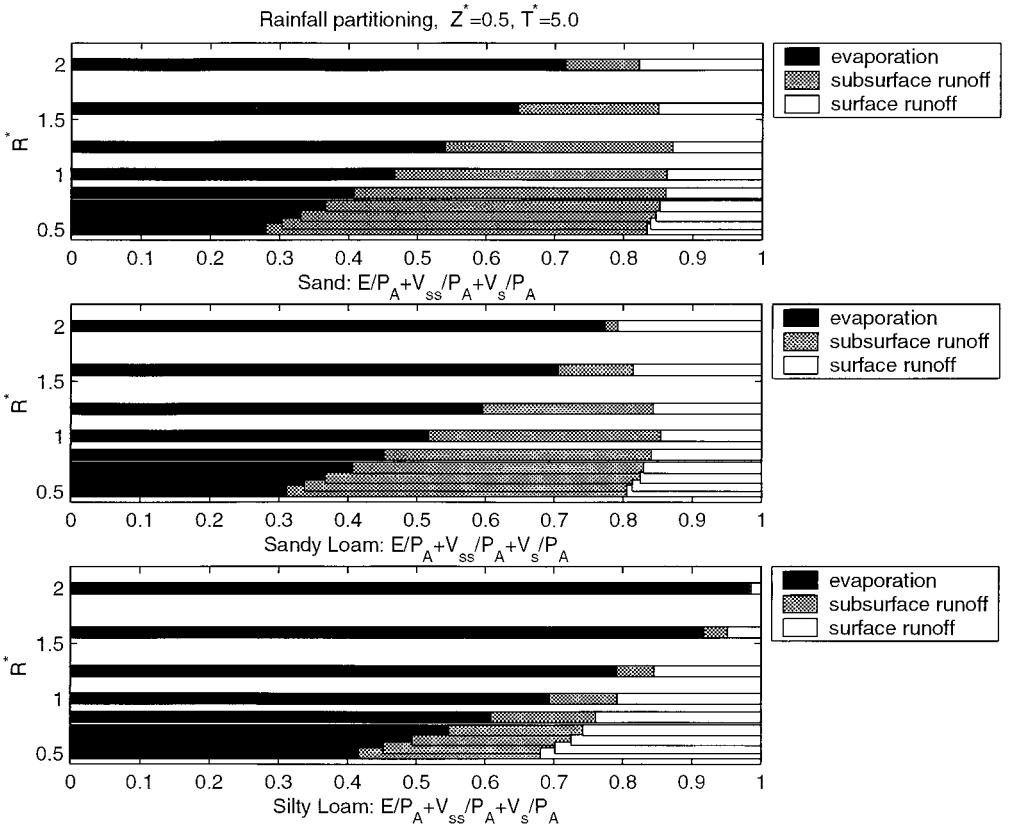

Figure 6c. Effect of climatic dryness on annual water balance partitioning.

Figure 7. From the numerical simulations we observe that a change in T^*, in contrast to previous results for Z^* and R^*, has a much smaller, almost negligible, impact on the overall water balance and the equilibrium values. The reason for the low impact of storminess is that the soil properties in this study have been chosen such that infiltration excess runoff is negligible even under intense storms and result in a decoupling of the intensity of storms (for reference, see (44)). For example, the hydraulic conductivity of silty loam is equivalent to 12.5 mm h^{-1}; rainfall intensities need to be much higher than this in short-duration storms for infiltration excess runoff to be produced. Consequently, the climatic, dryness index R^* is the more dominant climatic control factor under these circumstances.

7.4. Climate, Soil, and Topographic Interactions

The results discussed so far have been about the sensitivity of water balance partitioning to individual parameters, such as the dryness index R^*, while all other parameters have been kept constant. These can be generalized to look at the combined effect of these factors. In this section we look at the combined effect of the dryness index R^* and the flatness index Z^*, while fixing the storminess index to a value of $T^* = 5.0$; we will also present results only for sandy loams. We have already shown that T^* is the lesser of the climatic parameters in terms of importance, and the effect of soil type is easily understood and does not require additional simulations to make their effects clear.

The results presented below are all obtained based on a 9×9 matrix of values of R^* and Z^*. The numerical model was run for each of these 81 combinations, and the resulting matrix of values of key model outputs are used to produce contour plots for each output variable in the Z^*–R^* space. The output variables investigated are (1) equilibrium water table elevation y_o^*; (2) equilibrium soil saturation s_o^*; (3) ratio of annual actual evapotranspiration to annual rainfall E_A/P_A; (4) ratio of annual depth of subsurface runoff to annual rainfall V_{ss}/P_A; and (5) the ratio of annual depth of surface runoff to annual rainfall V_s/P_A. The results are presented in Figures 8a–8e.

Figure 8a is a contour plot of y_o^* which exhibits a strong dependence on Z^* and less strong dependence on R^*. As the watershed becomes flatter, that is, as Z^* increases, water table rises strongly. On the other hand, water tables are shallower in humid climates and deeper in arid climates. These results are intuitively obvious. Figure 8b is the contour plot of soil saturation s_o^*. The dependence on Z^* and R^* is almost exactly opposite to that of y_o^*. We see that s_o^* depends strongly on R^* and much less strongly on Z^*. We find that s_o^* decreases with increasing R^*, which is obvious, and decreases slowly with increasing Z^*, the explanation of which has been presented before. Figure 8c presents the contour plot of E_A/P_A. In this case, the primary control of E_A/P_A is R^*, whereas Z^* is much less important. We see that E_A/P_A decreases with increasing aridity, as measured by R^*, ranging from $<30\%$ in humid, steep watersheds to nearly 90% in flat, semiarid watersheds. Note that since combined runoff is complimentary to total actual evapotranspiration, total runoff will also be dependent strongly on R^* and less strongly on Z^*, decreasing from 70% in humid climates to 10% in semiarid climates. While combined runoff, actual evapotranspiration, as well as s^*, are all strongly dependent on R^* and much less on Z^*, the relation-

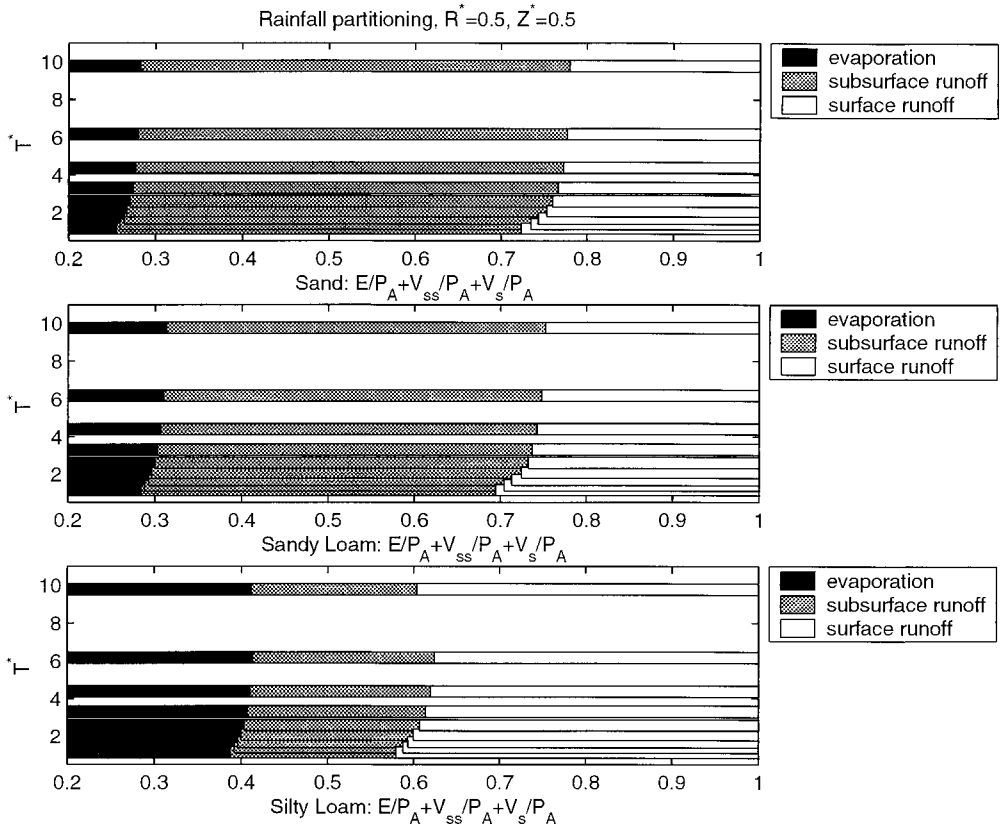

Figure 7. Effect of storminess on annual water balance partitioning.

ship between s^* and either evapotranspiration or combined runoff is not straightforward.

Figures 8d and 8e present contour plots of subsurface runoff V_{ss}/P_A and surface runoff V_s/P_A individually. They show that in contrast to actual evapotranspiration and combined runoff, V_{ss}/P_A and V_s/P_A are dependent on both R^* and Z^*. For example, subsurface runoff fraction, V_{ss}/P_A is, at ~50%, highest for humid, steep watersheds, and is nonexisting (0%) in flat, semiarid watersheds. On the other hand, V_s/P_A is, at 50%, highest for flat, humid (possibly tropical) watersheds and, at <15%, smallest in steep, semiarid watersheds. These are quite reasonable estimates in common hydrological experience and suggest that the numerical model is able to capture the essential features of annual water balance. They also suggest that while climate and soil properties appear to be the strongest determinants of combined runoff, and thus the partitioning of rainfall into runoff and evapotranspiration, the subsequent partitioning of total runoff into its surface and subsurface com-

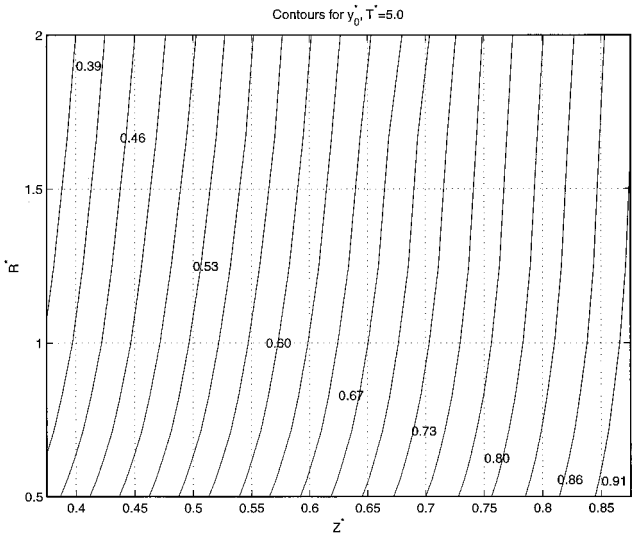

Figure 8a. Contours of equilibrium water table position.

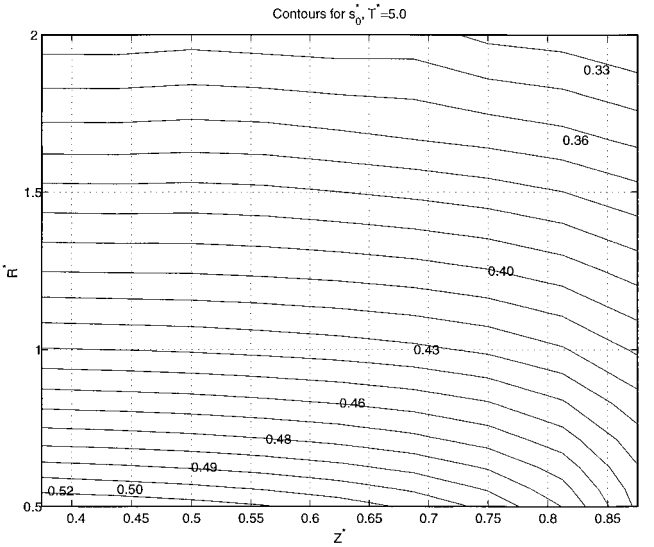

Figure 8b. Contours of equilibrium saturation value.

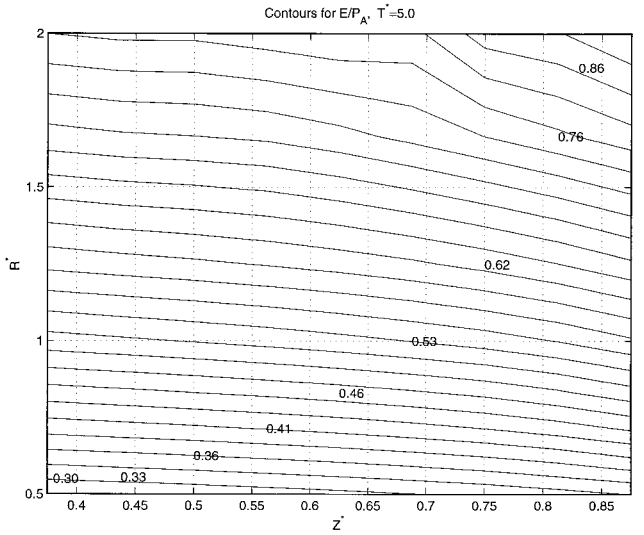

Figure 8c. Contours of cumulative annual evapotranspiration.

ponents is strongly dependent on topographic or landscape factors. This is an interesting result. It has implications for water balance modeling. So far, the only measurable watershed response has been combined runoff. It means that watershed models based on landscape features will not be easy to validate, unless more progress is made toward separating runoff into its surface and subsurface components, since it is only in this case that landscape factors begin to have a real impact. Recent advances in tracer hydrology should help to objectively separate the total runoff into its surface and subsurface components. This will lead to a better validation of our theory.

8. Summary

The work presented here explores the effects of physical controls on water balance for a hypothetical catchment entity, called representative elementary watershed (REW). For the analysis of flow we employed a system of conservation equations for mass and momentum for the unsaturated and saturated subsurface zones. These equations have been obtained by averaging microscale equations in space over the REW. The watershed-scale balance equations have been supplemented with constitutive relationships, governing mass fluxes and exchange of pressure forces between the unsaturated zone, the saturated zone, and the overland flow areas.

The governing equations have been cast into dimensionless form. In this way, we have identified significant dimensionless variables, parameters, and timescales, which allow us to classify hydrologic systems in a general manner based on their topography, soil properties, and atmospheric forcing.

We have developed a numerical model for solving the dimensionless governing equations, with realistic parameter values, and without any calibration whatsoever. We have obtained results which are consistent with common hydrological experience. In this modeling exercise we have systematically investigated the relative significance of a number of controls on annual water balance. For the examples studied here, climate (through the dryness index), topography (through the flatness index), and soil type are found to be most significant, while storminess has a smaller impact. Equilibrium water table elevations were found to be higher (closer to the soil surface) in poorly drained watersheds (flat, with less permeable soils) and lower in well-drained soils (steep, with permeable soils). Total annual evapotranspiration and runoff were strongly dependent on dryness index and much less on topographic factors (i.e., flatness index). On the other hand, topographic or landscape factors are important in the partitioning of total runoff into surface runoff and subsurface runoff.

The results presented above lend some credibility to our belief that the theoretical development of the governing equations, including the constitutive relations, are justified. However, we must emphasize that there are still a number of limitations in the theory, and in the numerical model, which need to be improved through future research. Aspects of watershed response that have not been considered include: detailed topographic features such as convergence and divergence, spatial variability of soils (horizontal as well as vertical, including layered soils), randomness of storm arrivals and storm duration, seasonality of both rainfall and potential evapotranspiration, and spatial variability of rainfall.

The most significant simplification has been that of evapo-

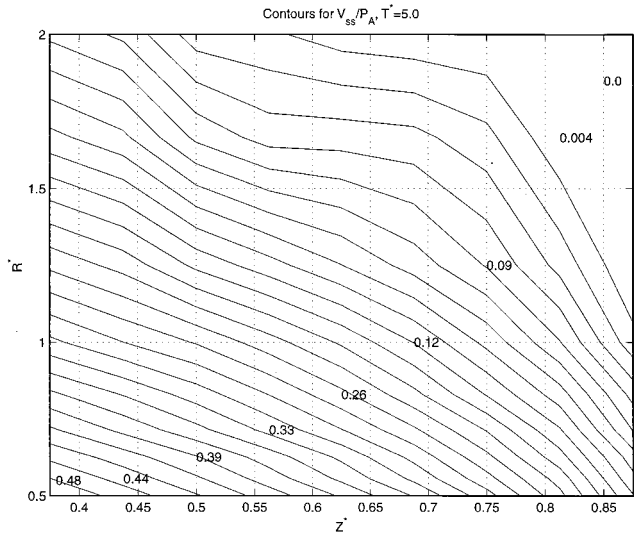

Figure 8d. Contours of cumulative annual subsurface runoff.

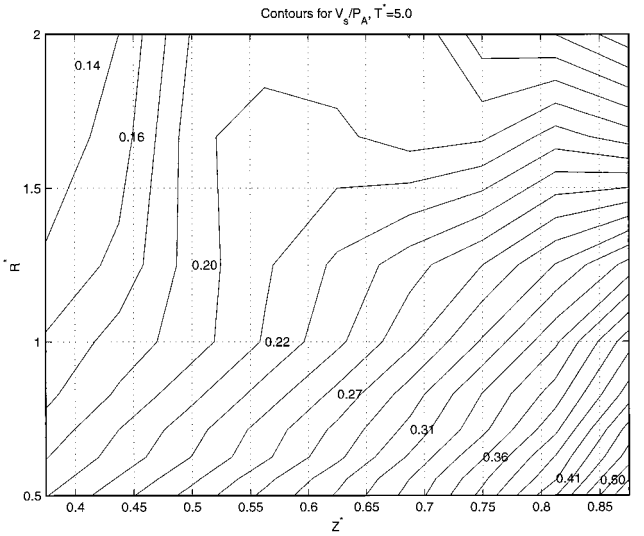

Figure 8e. Contours of cumulative annual surface runoff.

transpiration. The theoretical development has so far ignored explicit treatment of radiation exchange at the surface, the effect of plant roots and leaf canopies, the atmospheric boundary layer, and the water vapor transport in soils. This is left as a topic of further research. Also, constitutive relationships governing the mass fluxes such as infiltration, groundwater recharge, and discharge need to be improved through careful field experiments and/or grid-based numerical models which solve the partial differential equations governing flow in porous media.

9. Concluding Remarks

Lest this paper be misunderstood for what it is trying to achieve, we attempt here to give a broader perspective. Previously, *Reggiani et al*. [1998, 1999a] have developed a thermodynamic framework for the study of watersheds. This has involved deriving the balance equations for mass, momentum, energy, and entropy and the development of a rigorous constitutive theory based on the second law of thermodynamics.

For the theory to have utility for predictive models of watershed response, progress in three directions are required: (1) further theoretical derivations to include other subregions such as the atmospheric boundary layer, to include the vapor phase, and to make fundamental advances in the constitutive theory; (2) extensive field measurements combined with the use of detailed (small-scale) numerical models to develop appropriate parameterizations of sub-REW variability of soils, vegetation, and climatic variables; and (3) development and testing of numerical models based on the REW-scale balance equations and constitutive relations derived above.

Progress must be sustained in all three areas, in a balanced manner, and with the acknowledgment that each of the above tasks requires many years to accomplish. Field measurements cannot wait for the theory development to be complete, and modeling cannot wait for the other two tasks to be accomplished. To retain the credibility of the theory we propose, it is therefore important to demonstrate to a sceptical research community, at every step of the way, that the theory indeed has potential, i.e., will ultimately lead to predictive models of watershed response. This is what we have tried to achieve in this paper: a model based on the theory, albeit based on many simplifying assumptions, has already been able to make realistic simulations of annual water balance.

A number of concerns can then be raised; we discuss four. One legitimate concern in this regard is the validity of the many assumptions made in arriving at the final equations used in our model. However, what we present here is only a first step; we do not exclude that these assumptions can be relaxed in the future. For example, the proposed constitutive relationships can be replaced by more sophisticated expressions incorporating the effects of sub-REW variability. This will require much more work in terms of field experiments and fine-grid numerical modeling, as happens in any other field of science. Yet each time we make advances in the constitutive relations, the theory ensures that the laws of physics continue to be observed.

The second concern is that after all this theoretical work, we have only obtained well-known results, for example, the Darcy-like equations for flow in the unsaturated and saturated subsurface subregions of the REW, so there is nothing new. This is not entirely true, and even if it were so, it is not necessarily a weakness of the theory; if anything, it is just the opposite. First, what we have obtained is a REW-scale Darcy equation, not a point-scale equation. Second, in deriving these equations we have exposed the underlying assumptions, so that readers understand where the upscaled Darcy's law comes from. More importantly, there is little difficulty within our formalism to extend the theory to a second-order law to replace Darcy's law if the field situation dictates it. For example, if macropore flow is an important element of subsurface flow, current theories (such as Richards equation) will have difficulty accommodating it because of their reliance on Darcy's law. In our theory this is easily handled by postulating a second- or higher-order expansion of the friction force around the equilibrium (pressure) force. It is true that we did not introduce this generalization in this paper since we felt that it would be pointless without a parallel field investigation. That does not mean that it cannot be done or the approach itself is useless.

Third, we agree that an ad hoc postulation of constitutive relations, based purely on physical intuition rather than the second law, could presumably have led to similar results for the simple case we presented here. Nevertheless, we believe that postulating these exchange terms with the aid of a physical constraint, founded on a classical physical principle such as the second law of thermodynamics, is very valuable for problems where physical intuition does not exist or is suspect. There is a large body of literature in water resources, chemical engineering, and reservoir engineering in which researchers have applied various approaches only to obtain Darcy's law for fluid flow in porous media as their end result. Surely this has not been in vain and useless. The important question regarding each approach is whether it allows modeling a complex system in a rigorous manner. Indeed, the entropy inequality approach we use here has proven to be a powerful and invaluable tool for the analysis of porous media systems. For example, in the case of two-phase flow, when interfaces and their properties are taken into account, new forms of Darcy's law and capillary-pressure saturation relationships emerge [see *Hassanizadeh and Gray*, 1990]. In such a complex system the derivation of constitutive relationships by making ad hoc assumptions and without using the second law of thermodynamics as a constraint may lead to incomplete and/or unacceptable results. For this reason, we are confident that the use of the second law of thermodynamics forms a sound basis for the derivation of constitutive relationships in complex systems and should therefore be included into any theoretical formalism.

Finally, concerns can be raised about the value of the simple water balance model when so many simplifying assumptions have been used in its development, e.g., spatial and temporal homogeneity. In fact, it is a sign of confidence in the theory that even while the model is extremely simple, it is still able to produce very realistic water balance behavior in hypothetical watersheds. It can only improve from here, with future advances in field measurements and model parameterizations. While we await these developments, if we had not carried out such modeling, the theory will remain as a set of unproven governing equations, the applications of which will remain undemonstrated to the hydrologic community. This work is therefore a small step in a long road to the development of a new rigorous theory of hydrology at the watershed scale.

Appendix A: Parameterized Balance Equations

A1. Balance of Mass for the Unsaturated Zone

We introduce the linearized mass exchange terms (31), (32), and (36) into the mass balance equation (11) and obtain

$$\rho\varepsilon \frac{d}{dt}(s^u y^u \omega^u) = \min\left\{ \rho i \omega^u, \frac{\rho K_{\text{sat}} \omega^u}{\Lambda_u}\left[\tfrac{1}{2} y^u - \psi_b (s^u)^{-1/\mu}\right]\right\} \cdot \delta[0, t_r] + \rho\varepsilon\omega^u v^u - \rho\omega^u s^u e_p \delta[t_r, t_a], \quad \text{(A1)}$$

where the term on the left-hand side is storage, the first term on the right-hand side is infiltration, the second term is percolation/capillary rise, and the last term is evaporation. The function $\delta[a, b]$ is equal to 1 if the time t falls between a and b and is zero otherwise. Equation (A1) can be employed to evaluate the average saturation s^u.

A2. Balance of Momentum for the Unsaturated Zone

The conservation of momentum is derived from the general balance law (13), where the inertial term has been neglected. In section 3, equation (13) has been projected along the vertical direction. After substitution of the equilibrium force (39) and the linearized nonequilibrium resistance term (40) into (22) we obtain an integrated version of Darcy's law for unsaturated porous media flow:

$$-\varepsilon s^u y^u \omega^u \rho g + \varepsilon\rho g \omega^u s^u \left[\tfrac{1}{2} y^u - \psi_b (s^u)^{-1/\mu}\right] = -[K_{\text{sat}} (s^u)^{\lambda}]^{-1} \varepsilon \rho g y^u \omega^u v^u, \quad \text{(A2)}$$

where the first term on the left-hand side is gravity, the second term is the force acting on the water phase across the land surface, and the right-hand side term is the resistance acting on the water within the pores. Equation (A2) will be utilized to calculate the average velocity v^u within the unsaturated zone.

A3. Balance of Mass for the Saturated Zone

The mass balance for the saturated zone is obtained after substituting the respective mass exchange terms (32) and (33) into the balance equation (12):

$$\rho\varepsilon \frac{d}{dt}(y^s \omega^s) = -\rho\omega^u \varepsilon v^u - \frac{\rho K_{\text{sat}} \omega^o}{\cos(\gamma^o)\Lambda_s} \frac{1}{2}(y^s - z^r + z^s), \quad \text{(A3)}$$

where the left-hand side is storage, while the right-hand side terms represent percolation/capillary rise and outflow across the seepage faces, respectively. Equation (A3) will be utilized to calculate the average unsaturated zone depth y^u.

Appendix B: Geometric Relationships

The equation system presented in Appendix A is characterized by three equations in the seven unknowns v^u, s^u, y^u, y^s, ω^u, ω^s, ω^o. Four additional constitutive relationships are necessary to close the problem. Therefore we make the following four additional assumptions:

1. The entire REW is underlain by the saturated zone, yielding a constant area fraction for the saturated zone which is equal to unity, i.e., $\omega^s = 1$.

2. The sum of the volumes occupied by the unsaturated and the saturated zones is constant due to the fact that the two zones constitute competitive stores, which occupy an overall invariant portion of soil V. Division by the horizontal surface area projection Σ of the REW yields

$$y^u \omega^u + y^s = Z, \quad \text{(B1)}$$

where Z is the average total soil depth defined by V/Σ.

3. Next, we relate the seepage area fraction (or percentage of saturated REW surface area projection) ω^o to the average unsaturated zone depth:

$$\omega^o = \omega^o(y^s). \quad \text{(B2)}$$

This relationship can either be derived by making use of distributed models such as TOPMODEL or through field surveys and is strongly dependent on the local topographical circumstances. In the present application we approximate (B2) through a linear relationship between the two variables. The coefficients are found by imposing a zero seepage area ($\omega^o = 0$), when the average saturated zone depth coincides with the elevation of the channel ($y^s = z^r - z^s$) and $\omega^o = 1$ for a totally saturated subsurface zone ($y^s = Z$, $y^u = 0$):

$$\omega^o = \beta^{\omega}(y^s - z^r + z^s), \quad \text{(B3)}$$

where β^{ω} is an appropriate proportionality constant, defined as

$$\beta^{\omega} = \frac{1}{(Z - z^r + z^s)}. \quad \text{(B4)}$$

4. Finally, the unsaturated and saturated catchment areas are complementary, adding up to unity, neglecting the channel area fraction. Consequently, we obtain that

$$\dot{\omega}^u = -\dot{\omega}^o. \quad \text{(B5)}$$

These four additional geometric relationships allow us to overcome the deficit of four equations in the system.

Notation

$\mathcal{A}$	linearization parameter for the mass exchange terms $[T/L]$.
$\mathcal{B}$	linearization parameter for the mass exchange terms $[M/L^3]$.
$\mathbf{e}_x$, $\mathbf{e}_y$, $\mathbf{e}_z$	unit vectors pointing along the x, y, and z axes, respectively.
e_p	potential rate of evaporation $[L/T]$.
$\mathbf{g}$	gravity vector $[L/T^2]$.
i	mean rainfall intensity $[L/T]$.
K_{sat}	saturated hydraulic conductivity $[L/T]$.
p^s, p^u	water pressure in the saturated and unsaturated zones $[F/L^2]$.
p_{cap}	average capillary pressure, $[F/L^2]$.
R	soil resistivity, defined as K^{-1} $[T/L]$.
s^u	saturation function for the unsaturated zone [dimensionless].
S	surface area of the REW $[L^2]$.
t	time $[T]$.
t_b	interstorm period $[T]$.
t_r	storm period $[T]$.
t_a	climatic period $t_r + t_b$ $[T]$.
$\mathbf{T}$	force exchanged per unit surface area projection $[M/T^2L]$.
$\mathbf{v}$	velocity vector of the bulk phases $[L/T]$.
V	volume occupied by the subsurface zone $[L^3]$.
y^j	average thickness of the j subregion along the vertical $[L]$.
z^r	average elevation of channel bed with respect to datum $[L]$.

z^s average elevation of the bottom surface of the REW with respect to datum $[L]$.
z^c average elevation of the unsaturated portion of the land surface with respect to datum $[L]$.
z^o average elevation of seepage face with respect to datum $[L]$.
Z average thickness of the subsurface zone, defined in Appendix B $[L]$.
γ^o slope angle of the overland flow plane with respect to the horizontal.
$\delta[a, b]$ generalized function, which is nonzero over the interval between brackets.
ε soil porosity [dimensionless].
λ pore-disconnectedness index.
Λ typical length scale for infiltration or seepage outflow $[L]$.
μ pore size distribution index.
ζ^j elevation of the center of mass of a subregion with respect to a datum $[L]$.
ρ water mass density $[M/L^3]$.
Σ projection of the total REW surface area S onto the horizontal plane $[L^2]$.
Σ^u, Σ^o area projection covered by the unsaturated zone or the overland flow $[L^2]$.
ψ_b bubbling pressure head $[L]$.
ω^u, ω^o saturated and unsaturated surface area fractions [dimensionless].

Acknowledgments. We would like to thank David Tarboton, Christopher Duffy, Ross Woods, and an anonymous reviewer for their constructive comments, which have contributed to a significant improvement of the manuscript. P. Reggiani was supported by an Overseas Postgraduate Research Scholarship (OPRS) offered by the Department of Employment, Education and Training of Australia and by a University of Western Australia Postgraduate Award (UPA). Centre for Water Research Reference ED 1463 PR.

References

Bras, R. L., *Hydrology—An Introduction to Hydrologic Science*, Addison-Wesley-Longman, Reading, Mass., 1990.

Brooks, R. H., and A. T. Corey, Properties of porous media affecting fluid flow, *J. Irrig. Drain. Div. Am. Soc. Civ. Eng.*, *IR2*, 61–88, 1966.

Burdine, N. T., Relative permeability calculations from pore size distribution data, *Trans. Am. Inst. Min. Metall. Pet. Eng.*, *198*, 71–78, 1958.

Coleman, B. D., and W. Noll, The thermodynamics of elastic materials with heat conduction and viscosity, *Arch. Ration. Mech. Anal.*, *13*, 168–178, 1963.

Duffy, C. J., A two-state integral-balance model for soil moisture and groundwater dynamics in complex terrain, *Water Resour. Res.*, *32*(8), 2421–2434, 1996.

Dunne, T., Field studies of hillslope flow processes, in *Hillslope Hydrology*, edited by M. J. Kirkby, pp. 227–293, John Wiley, New York, 1978.

Eagleson, P. S., Climate, soil and vegetation, 1, Introduction to water balance dynamics, *Water Resour. Res.*, *14*(5), 705–712, 1978a.

Eagleson, P. S., Climate, soil and vegetation, 4, The expected value of annual evapotranspiration, *Water Resour. Res.*, *14*(5), 731–739, 1978b.

Eagleson, P. S., Climate, soil and vegetation, 6, Dynamics of the annual water balance, *Water Resour. Res.*, *14*(5), 749–764, 1978c.

Eagleson, P. S., Climate, soil and vegetation, 7, A derived distribution of annual water yield, *Water Resour. Res.*, *14*(5), 765–776, 1978d.

Hassanizadeh, S. M., and W. G. Gray, Mechanics and thermodynamics of multiphase flow in porous media including interphase boundaries, *Adv. Water Resour.*, *13*(4), 169–186, 1990.

Hawk, K. L., and P. S. Eagleson, Climatology of station storm rainfall in the continental United States: Parameters of the Bartlett-Lewis and Poisson rectangular pulses models, technical report, Ralph M. Parsons Lab., Dep. of Civ. and Environ. Eng., Mass. Inst. of Technol., Cambridge, 1992.

Milly, P. C. D., Climate, soil water storage, and the average annual water balance, *Water Resour. Res.*, *30*(7), 2143–2156, 1994.

Press, W. H., S. A. Teukolsky, W. T. Vetterling, and B. P. Flannery, *Numerical Recipes in C*, Cambridge Univ. Press, New York, 1992.

Reggiani, P., M. Sivapalan, and S. M. Hassanizadeh, A unifying framework for watershed thermodynamics: Balance equations for mass, momentum, energy and entropy, and the second law of thermodynamics, *Adv. Water Resour.*, *22*(4), 367–698, 1998.

Reggiani, P., S. M. Hassanizadeh, M. Sivapalan, and W. G. Gray, A unifying framework for watershed thermodynamics: Constitutive relationships, *Adv. Water Resour.*, *23*(1), 15–39, 1999a.

Reggiani, P., M. Sivapalan, S. M. Hassanizadeh, and W. G. Gray, Coupled equations for mass and momentum balance in a bifurcating stream channel network: Theoretical derivation and numerical implementation, *Rep. ED 1266 PR*, Cent. for Water Res., Univ. of West. Aust., Nedlands, 1999b.

Robinson, J. S., and M. Sivapalan, Temporal scales and hydrologic regimes: Implications for flood frequency scaling, *Water Resour. Res.*, *33*(12), 2981–2999, 1997.

Salvucci, G. D., and D. Entekhabi, Comparison of the Eagleson statistical-dynamical water balance model with numerical simulation, *Water Resour. Res., 30*(10), 2751–2757, 1994.

Salvucci, G. D., and D. Entekhabi, Hillslope and climatic controls on hydrologic fluxes, *Water Resour. Res.*, *31*(7), 1725–1739, 1995.

S. M. Hassanizadeh, Section for Hydrology and Ecology, Faculty of Civil Engineering and Geosciences, Delft University of Technology, P.O. Box 5048, 2600 GA Delft, Netherlands.

P. Reggiani and M. Sivapalan, Centre for Water Research, Department of Environmental Engineering, University of Western Australia, Nedlands, Western Australia 6907, Australia. (sivapalan@cwr.uwa.edu.au)

(Received July 9, 1999; revised March 3, 2000;
accepted March 10, 2000.)